buildings

MDPI

Article

Effect of Spacing and Slenderness Ratio of Piles on the Seismic Behavior of Building Frames

Joseph Antony Visuvasam [1,*] and Sembulichampalayam Sennimalai Chandrasekaran [2]

[1] School of Civil Engineering, Vellore Institute of Technology, Vellore 632014, India
[2] Centre for Disaster Mitigation and Management, Vellore Institute of Technology, Vellore 632014, India
* Correspondence: visuvasam.j@vit.ac.in; Tel.: +91-9894264192

Abstract: The general assumption of a rigid base at the bottom of building structures during analysis and design underestimates the seismic response. Building structures resting on loose sand and soft clayey soil are vulnerable to earthquake forces. The amplification of ground motion occurs due to the presence of this loose and soft soil deposit. Moreover, the spacing and slenderness ratio of piles play a vital role in altering the behavior of the overall soil-foundation-superstructure system. This study aimed at investigating the effect of soil-pile-structure interaction using 1-g shake-table testing. Free and forced vibration tests were performed on scaled building frames with either a rigid base or a flexible base, supported on sandy soil with 50% relative density. A laminar shear box container is used for an experimental study of soil-pile-structure interaction. The design parameters, such as the spacing (S = 3D, 5D, 7D, and 9D) and slenderness ratio (L/D = 15, 30, 45, and 60) of the piles, where S, D and L are spacing, diameter and length of the piles respectively, are considered in the analysis. The results, in terms of natural frequency, damping, pile-bending moment, story lateral displacement, and inter-story drift are estimated. From the findings, it is clear that the effects due to pile spacing are more considerable than the effects due to the slenderness ratio of the piles. The bending moment in the piles spaced at 3D is increased by 102% compared to the large-spacing (S = 9D) piles. This subsequently amplifies the story lateral displacement by 180% and amplifies the inter-story drift by 167%.

Keywords: shake table testing; pile spacing; slenderness ratio; natural frequency; bending moment; inter-story drift

Citation: Visuvasam, J.A.; Chandrasekaran, S.S. Effect of Spacing and Slenderness Ratio of Piles on the Seismic Behavior of Building Frames. *Buildings* **2022**, *12*, 2050. https://doi.org/10.3390/buildings12122050

Academic Editor: Silvia Costanzo

Received: 26 October 2022
Accepted: 17 November 2022
Published: 23 November 2022

1. Introduction

Pile foundations are generally used to support bridges, offshore wind turbines, jacketed platforms, transmission towers, high-rise buildings, and the vibratory machines that are used in power plants and petrochemical complexes. Moreover, they are used in coastal regions, where the majority of the sites are covered with weak clays, marine deposits, and loose sandy soils [1,2]. These pile foundations are often required to resist lateral loads and moments, in addition to axial compressive or tensile forces [3]. The resistance along the horizontal direction depends on the type of the surrounding soil and pile group configuration. In addition, the behavior of pile groups under lateral dynamic loads is non-linear and complex in nature. According to Reese et al. [4], the behavior of a pile group that is subjected to dynamic lateral loads is different from that of a single pile. The lateral resistance of the pile group is reduced, due to pile-soil-pile interaction. The bending moment development in closely spaced piles (3D, where D is diameter of pile) is increased by 20%, due to group interaction [5]. Moreover, the various other factors that affect the lateral behavior of pile foundations are the spacing of piles, the number of piles in a group, the configuration of the pile group, soil stiffness, flexural rigidity, the slenderness ratio of the piles, and the fixity conditions at the pile head. In addition, the group's interactions owing to the degradation of soil stiffness increased the bending moment and deflection of the pile group more than

that of single piles subjected to the same average load [6,7]. In a recent study [8], it was found that the natural frequencies of single and grouped helical piles decreased due to successive shaking. This results in large soil deformation and a reduction in the stiffness of the soil-pile system, due to the occurrence of resonant conditions. Therefore, appropriate consideration is required in an investigation of the analysis and design of piles under horizontal dynamic actions, taking into account soil-pile-structure interaction (SPSI).

Superstructures are generally assumed to be fixed or rigid for the purposes of seismic analysis and design. In reality, the soil-foundation system that is present beneath ground level affects the superstructure response significantly. The behavior of the substructure is affected by the behavior of the superstructure and vice versa; this phenomenon is called soil–structure interaction (SSI). Ignoring SSI during seismic analysis means that it cannot effectively simulate the actual scenario of wave propagation and transfer mechanisms in the superstructure [9]. According to a previous study [10], the soil–foundation system's response increases the natural time-period and ductility demands of the overall system. Determining the response of structures when taking into account SSI effects also requires the simulation of both inertial and kinematic interaction. The effects are small for light and flexible structures that are resting on firm ground. However, the effects are detrimental to rigid structures resting on soft soils. Ground motions may increase the spectral accelerations because of the amplification of the ground acceleration and fault rupture directivity effects [11]. Previously published research [12–14] suggests that the SSI effects are considerable when a structure is founded on soft soil and the shear wave velocity is less than 600 m/s.

The significance of soil-pile-structure interaction to the failure of various structures was evidenced by post-earthquake investigations detailed by several researchers [15–22]. The majority of buildings and bridges standing during the 1964 Niigata earthquake [18], the 1985 Mexico earthquake [19], the 1995 Kobe earthquake [20], and the 2001 Bhuj earthquake [21] were severely damaged due to the effects of soil-pile-structure interaction. The superstructures that were supported on soil-pile mediums experienced large lateral displacements and inter-story drift values [23–26] in comparison with rigid-base superstructures. The rise in response parameters is due to the amplification of acceleration by the presence of flexible soil deposits. Moreover, the response of the building depends on the selection of a suitable soil profile [27], amplification factors, and the target spectrum of the site [28]. However, the pile group interaction reduces the resistance of the soil medium by degrading the soil stiffness. This clearly demonstrates the importance of considering the SPSI in the analysis and design of the overall system when subjected to seismic forces.

Field testing of soil-foundation-structure systems has been carried out over the past few decades to investigate the significance of SSI. The study included static lateral loading, cyclic loading, and dynamic loading using various foundations. The primary outcome of the response parameters of all these studies was the stiffness and damping functions. Static lateral loads were applied to single and different configurations of pile groups [7,29–36]. Similarly, cyclic lateral loadings [37–44], dynamic lateral loadings [45–48], and small-scale field testing [49–53] were carried out by various researchers.

The experimental testing of scaled models in geotechnical applications is performed either by using shake-table tests or centrifuge tests. These testing results are generally used for the quantitative prediction of numerical and analytical results. Various researchers [54–56] have considered the superstructure as a single-degree-of-freedom system for the shake-table tests. The drawback of such tests is that the superstructure's flexibility may not be accounted for and the effect of higher modes would not be considered in the entire soil-foundation-structure study. In addition, the ignoring of the superstructure in soil-structure interaction studies may not allow the capture of the inertial force transfer mechanism. In addition, the soil-foundation system alters the natural time period, which ultimately changes the spectral acceleration of the building. This results in changes to the base shear and lateral story displacements. The effects of SSI on a natural time period in terms of low- to high-rise RC buildings have been proposed in the form of empirical relationships by

various researchers [57–59]. Very few researchers [60–63] have considered superstructure as a building model for shake-table testing and studied the seismic response.

In summary, post-earthquake investigations reveal that the soil-pile-structure interaction influences the superstructure's behavior detrimentally. In actual practice, ignoring SSI and SPSI during the analysis and design of the foundation and superstructure may cause either the underestimation or over-estimation of the response parameters. Over the past few decades, experimental and numerical investigations were carried out to address the effects of SSI on the overall soil-foundation-superstructure system. Very limited works [23,60,61] are available that consider the superstructure in the context of SPSI investigations. Thus, in this study, a building model for the superstructure is presented that demonstrates the structure's characteristics, such as natural frequency, density, and the number of stories in the prototype superstructure. Furthermore, a laminar shear box is employed to simulate the free-field behavior of the soil medium. The model pile cap and pile foundations have been designed to represent the prototype foundations. Design parameters, such as the spacing and length of the pile foundations, have been varied for the study. Finally, experimental tests are performed on a rigid-base and soil-pile-supported superstructure, and the results are compared.

2. Description of Prototype Structural Models

2.1. Superstructure

The considered superstructure for this experimental study is a conventional seven-story reinforced concrete building frame, with an overall height of 28 m and a base dimension of 8 m, comprising two spans. The dead loads [64] and imposed load of 4 kN/m^2 [65] are adopted, as per the Indian Standards for buildings. The superstructure is analyzed, adopting the seismic parameters according to the figures in [66]. The building is assumed to be located in Vellore city, India; hence, the zone factor (Z) is 0.16. The functional use of the structure is residential, and the response reduction factor (R) is adopted as 5. The damping of the building is assumed to be 5%. The soil type is considered to be a medium. The grade of concrete and grade of reinforcement steel adopted for the design of the superstructure are M30 and Fe415, respectively. The natural frequency of the fixed-base prototype superstructure is established to be 0.49 Hz. The building is designed according to a previous study [67], using the structural analysis programming tool, SAP2000 (version.19.2, CA, USA) [68].

2.2. Soil

The specific gravity (G_s) of the sandy soil was estimated in the laboratory using the Pyconometer method, according to the authors of [69], and was established to be 2.64. The relative density test was conducted as per [70] and the values of maximum (ρ_{max}) and minimum dry density (ρ_{min}) of the sandy soil are established as 1.77 g/cc and 1.52 g/cc, respectively. A direct shear test was performed, as per [71], and the value for the angle of internal friction (ϕ) of the soil corresponding to the 50% relative density was obtained, at 35°. A dry sieve analysis was performed, according to the procedure in [72], to evaluate the grain-size distribution of the soil. The sandy soil was classified as poorly graded sand (SP), as per the Indian Standard [63] and Unified Soil classification systems [73]. The experimental building rested on a pile cap and pile foundations. The grades of concrete and reinforcement steel used for the design of the pile cap and pile foundations were M25 and Fe415, respectively. The total width of the pile cap in both the x and y directions was 12 m, and the thickness was estimated to be 700 mm. The pile foundations were designed for 3 × 3 pile group configurations, with various pile lengths (L) of 15D, 30D, 45D, and 60D and a pile spacing (S) layout of 3D, 5D, 7D, and 9D. The pile foundations were assumed to be of the floating/friction type, and the design was carried out according to the model in [74]. The prototype superstructure and the foundations were scaled according to the scaling law given in Table 1 and Equation (1), in order to obtain the models, and the test was performed using a shake table.

Table 1. The parameters used for scaling after Wood et al. [75].

Length (mm)	Density (kg/m^3)	Volume (m^3)	Stiffness (N/m)	Frequency (Hz)
1/n	1	$1/n^3$	$1/n^2$	$n^{1/2}$

3. Testing Facilities Used

3.1. Shake Table

Shake tables are generally used to quantify the behavior of soil, foundations, and structural models subjected to dynamic loading, especially earthquakes. The table is agitated with the help of hydraulic actuators to simulate the various types of periodic and transient motions. The shake table available at the Advanced Strength of Materials laboratory in the Vellore Institute of Technology, Tamil Nadu, India has a payload capacity of 1 MT. The base dimension of the shake table platform is 1 m $\times$ 1 m. The operating frequency of the shake table is limited to between 0.05 Hz and 20 Hz. The table can be excited to a maximum displacement of $\pm$ 150 mm. The model structure can be fixed to the table using M38 bolts.

3.2. Laminar Shear Box Container

Numerous researchers [23,54–56,58,76–85] have reported that a laminar shear box soil container can effectively capture the free-field response of soil during seismic excitation. Compared to rigid and flexible soil containers, laminar shear soil containers have been widely used for various studies [23,54,77] on SSI problems. The selection of the longitudinal, lateral, and vertical dimensions of the box must be based on the response of soil-structure systems that are not affected by the deformation that occurs during gravity and lateral loading. According to a previous study [86], the minimum longitudinal and lateral dimensions of the container should be five times the length along shaking direction and three times the width of the superstructure, respectively. Similarly, to prevent deformation of the soil, which can be attributed to the lateral and vertical loading, the container's minimum height should be greater than 1.5 to 2 times the length of the pile foundations [87]. Therefore, based on the available base dimensions of the shake table, the longitudinal, lateral, and vertical inner dimensions of the soil container were fixed at 900 mm, 600 mm, and 1000 mm, respectively.

The soil container was made of rectangular aluminum hollow sections with dimensions of 50 mm $\times$ 50 mm. The frames were separated with a gap of 5 mm by using rollers attached to the bottom of the frames. These rollers are employed to simulate the movement of soil layers during vibrations. Furthermore, to achieve the frictionless movement of the aluminum frames during loading, the sidewalls of the frames parallel to the loading direction were attached with a vertical steel frame using rollers. Indian Standard Angle sections (ISA) were used to make the vertical frame. This vertical steel frame is used to hold and position the rectangular aluminum frames before applying seismic excitation. The vertical frames and the rectangular aluminum frame were attached to the 20 mm-thick aluminum base plate. Finally, the entire arrangement was fixed to the shake table platform using six M38 bolts. The container was covered inside it, using a silicon rubber sheet of the required dimensions to hold the soil. Moreover, it was possible that the seismic waves passing through the soil medium may have reflected back during vibration. Hence, to avoid boundary effects when shaking the table, 25 mm-thick polystyrene foam panels were placed at the ends of the container, which were perpendicular to the loading direction. This arrangement is similar to those used in previous studies [58,88–90].

3.3. Instrumentation and Data Acquisition System

The performance of the overall SPSI system under seismic loading was obtained using various measuring instruments. The lateral story displacement of the superstructure was measured using displacement transducers (Figure 1a). HBM (Hottinger Baldwin Messtechnik Gmbh, Darmstadt, Germany) plunger-type displacement transducers (WA-L/200 mm)

with a nominal sensitivity of 80 mV/V (0.08 mm) were used. The strain gauges (Figure 1b) were installed along the length of the pile to obtain the strain that developed at the time of testing. HBM (Hottinger Baldwin Messtechnik Gmbh, Darmstadt, Germany) linear (1-LY11-3/120) strain gauge with normal resistance of 120 ± 0.5 ohms is used. The grid length and gauge factor are 3 mm and 2.02, respectively. The measured values were then converted into bending moments. All the measuring instruments (displacement transducers and strain gauges) were calibrated before beginning the shake-table testing. Two data acquisition systems, such as the HBM (Hottinger Baldwin Messtechnik Gmbh, Darmstadt, Germany) MX840B-Quantum X (8 channels) (Figure 1c), and a National Instruments system (c-DAQ 9178, Austin, Texas) (32 channels—see Figure 1d) were utilized in this testing program.

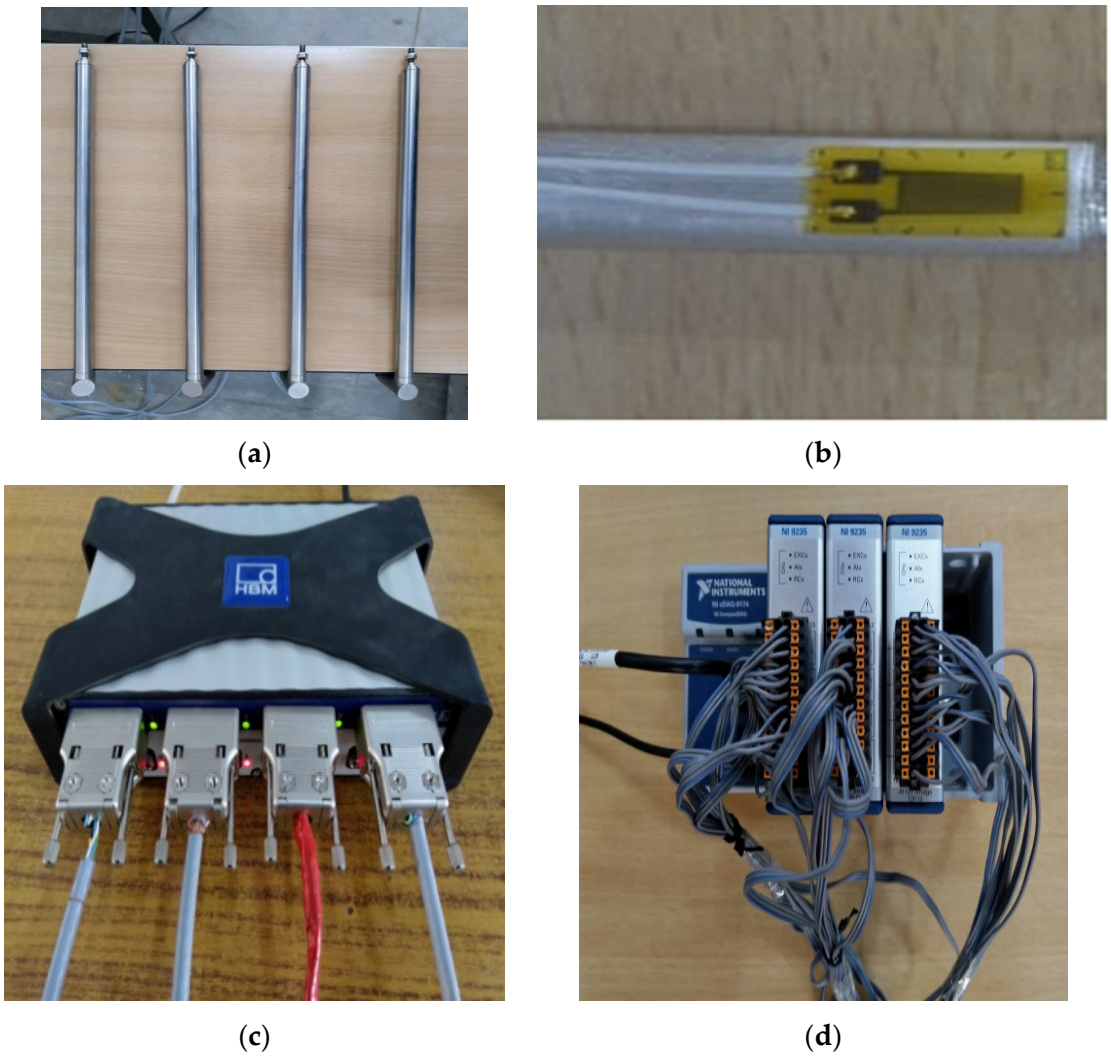

Figure 1. The instrumentation used for measuring the structural response: (**a**) linear variable displacement transducer, (**b**) linear strain gauge, (**c**) data acquisition system MX840B—HBM, and (**d**) a data acquisition system made by National Instruments.

4. Description of Scaled Models

4.1. Building Model

Scaled models used for experimental investigations should simulate the prototype's behavior during the shake-table test. Hence, to achieve a reliable scaled model representing the prototype's behavior, appropriate scaling factors are required [19]. Moreover, the geometric, kinematic, and dynamic similarities of the prototype and scaled models should be taken into consideration [91]. Considering the limitations of the available shake table and

the laminar soil container specifications, a scaling factor of 1:40 was adopted in the current experimental study. The scaling law used for the conversion of prototype superstructure and foundations into scaled models is presented in Table 1.

According to the scaling law recommended by the authors of [75], the frequency of the scaled superstructure model should be 3.10 Hz. The dimensions of the prototype building members should also be scaled. In addition, the required scaled stiffness of the column and weight of the structural model, calculated without the base plate, needed to be 34.33 N/m and 14.41 kg, respectively. The length, width, and height of the structural model were computed as 200 mm, 200 mm, and 700 mm, respectively. The calculation for the scale model's dimensions is given in Appendix A. The fabricated scaled superstructure model and the joint details are shown in Figure 2.

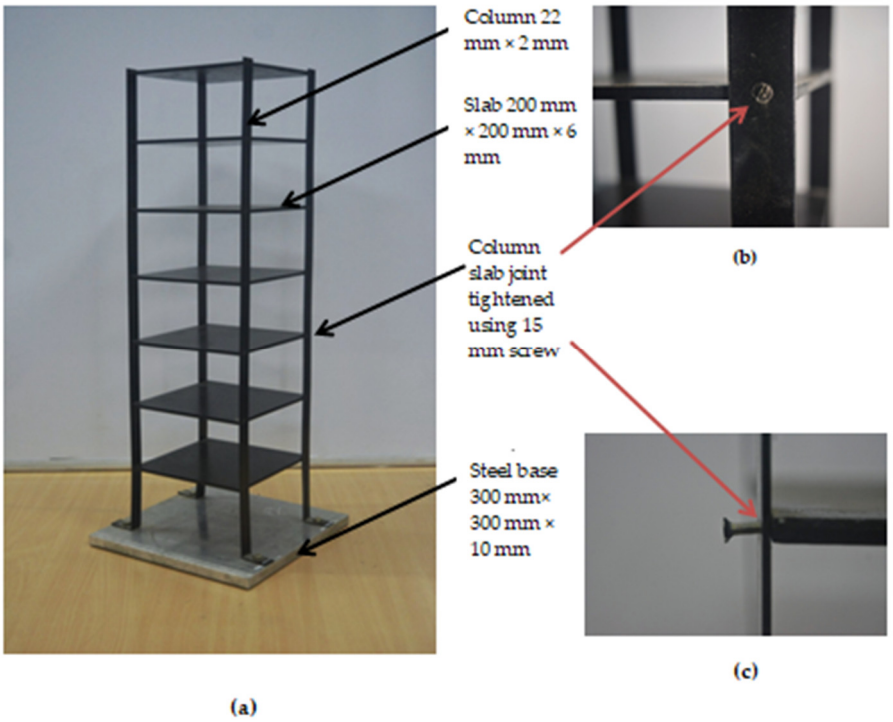

Figure 2. Fabricated scaled superstructure model: (**a**) overall view, (**b**,**c**) joint details.

The model has seven steel plates, sized 200 mm × 200 mm × 6 mm, to represent the floors, and four steel plates, sized 700 mm × 22 mm × 2 mm, to represent the columns. Steel-plate grade Fe410, manufactured according to Indian standards [92], with a minimum yield stress of 250 MPa and a minimum tensile strength of 410 MPa, has been adopted in the design. A steel plate of dimension 300 mm × 300 mm × 10 mm is placed at the bottom of the model, to act as a base plate. Holes are provided at 100 mm c/c to connect the unit with a shake table. The steel columns are attached to the plate at the bottom of the model, using M8 bolts. Similarly, the columns and steel floor plates are connected using 1.5 mm-diameter stainless steel metal screws with a length of 15 mm. Holes are provided at the locations of columns and slab joints.

4.2. Soil

The particle size distribution curve of the soil sample used for the scaled model experimental investigation is given in Figure 3. A poorly graded sandy soil (SP) with a mean diameter (D_{50}) of 0.34 mm is used for the experimental work. According to previous studies [93,94], the diameter of the model piles must be less than 20 times the effective grain size diameter, to avoid scale effects. Thus, the required effective grain size to reduce the scale error must be less than 0.4 mm. In this study, the effective mean diameter used is 0.34 mm, which is less than the required value of 0.4 mm; thus, the error can be minimized.

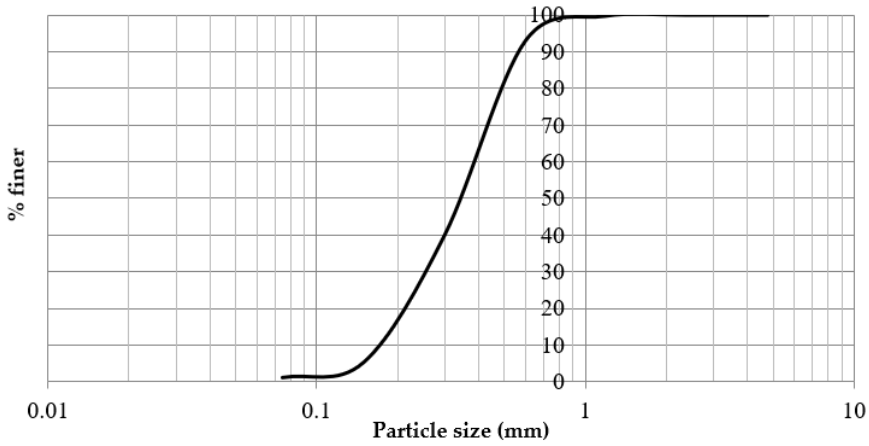

Figure 3. Particle size distribution curve of the soil employed for testing.

The soil was poured in until it reached the required quantity in the laminar shear box container for a D_r of 50%. Sand of the required weight was calculated and poured inside the soil container in various layers. The thickness of each soil layer was 75 mm. The soil bed was first prepared up to the bottom of the pile group system. After aligning the entire instrumented pile group and pile cap arrangement carefully in the required position, the remaining soil was poured in up to the top of the pile group system. Moreover, polystyrene foam of 25 mm thickness was positioned at the same time on either side of the laminar shear box, along the loading direction, to act as absorbent boundaries. Once the preparation of the soil bed was completed, the model superstructure was fixed at the pile cap level, using M8 bolts. Later, the displacement transducers were fixed to alternate story levels, comprising the roof (seventh), fifth, third, and first levels, and ensured a zero reading in the data acquisition system.

4.3. Model Foundations

Similar to the model structure, the scaling law is used to convert the prototype pile cap and pile into the model's foundations. It is necessary to consider those factors that affect the scaling of model foundations. According to a previous study [19], these factors are flexural rigidity (*EI*), slenderness ratio (*L/D*), relative stiffness, and the type of yield mechanism (rigid or flexible). In the present study, the flexural rigidity of the prototype pile foundations was scaled according to Equation (1) [75] as follows:

$$\frac{(EI)_p}{(EI)_m} = n^{4+\alpha} = n^{4.5} \quad (1)$$

where L and D are the length and diameter of the pile, respectively, $(EI)_p$ and $(EI)_m$ are the flexural rigidity of the prototype and model pile, respectively, E_p and E_m are the elastic modulus of the prototype and model pile material, respectively, I_p and I_m are the moments of inertia of the prototype and model pile, respectively, n is the scale factor, and α is the factor that depends on small-strain stiffness, which is equal to 0.5 for sand [75].

A total of nine piles with a 3 × 3 pile-group configuration was chosen. The behavior of the pile under lateral loading is based on the type of yield mechanism. According to previous research [74], the pile foundations are classified as rigid, intermediate, and flexible (elastic), based on their rigidity. In the present study, piles are designed to behave in the intermediate to the flexible range. Previous researchers [54,78,90,95,96] have used various types of materials, such as aluminum tubes, steel bars, and reinforced concrete to design pile models. Considering the scaling factor of 1:40 and the criteria of yield mechanism and the stiffness of piles, the required diameter of an aluminum solid section model pile is 8 mm. Moreover, an aluminum plate of 16 mm thickness with a 300 mm × 300 mm plan dimension is used for the pile cap. The pile foundations are instrumented, using strain

gauges fixed at the front, middle and rear rows of piles (Figure 4a). The numbers of strain gauges (Figure 4b) used for the various lengths of pile foundations are 4, 5, 7, and 8 for the lengths of 15*D*, 30*D*, 45*D*, and 60*D*, respectively.

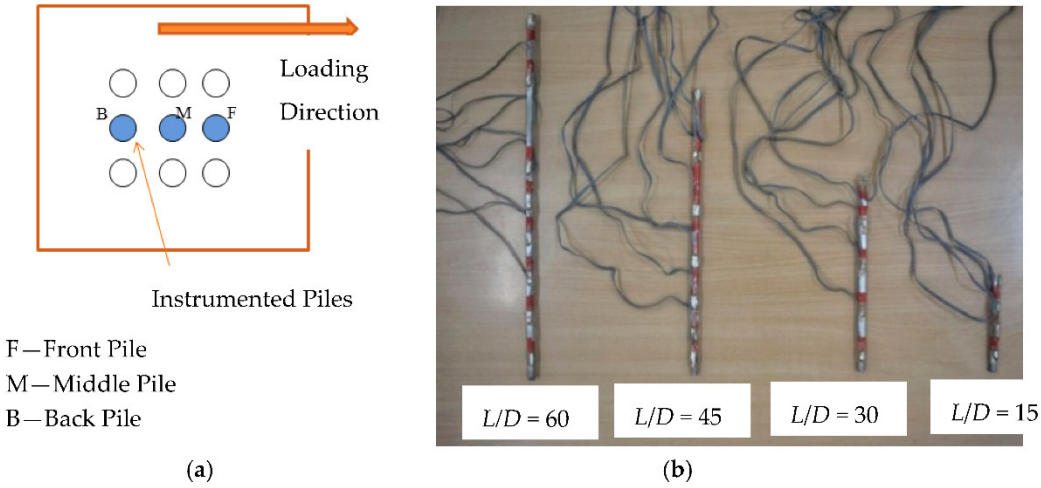

Figure 4. Instrumentation details: (**a**) details of the instrumented pile foundations, and (**b**) model piles with the strain gauges.

The displacement transducers are attached at the roof (seventh), fifth, third and first floors of both rigid- and flexible-base structural models. The overall arrangements of the rigid-base and soil-pile-supported models are shown in Figures 5 and 6, respectively.

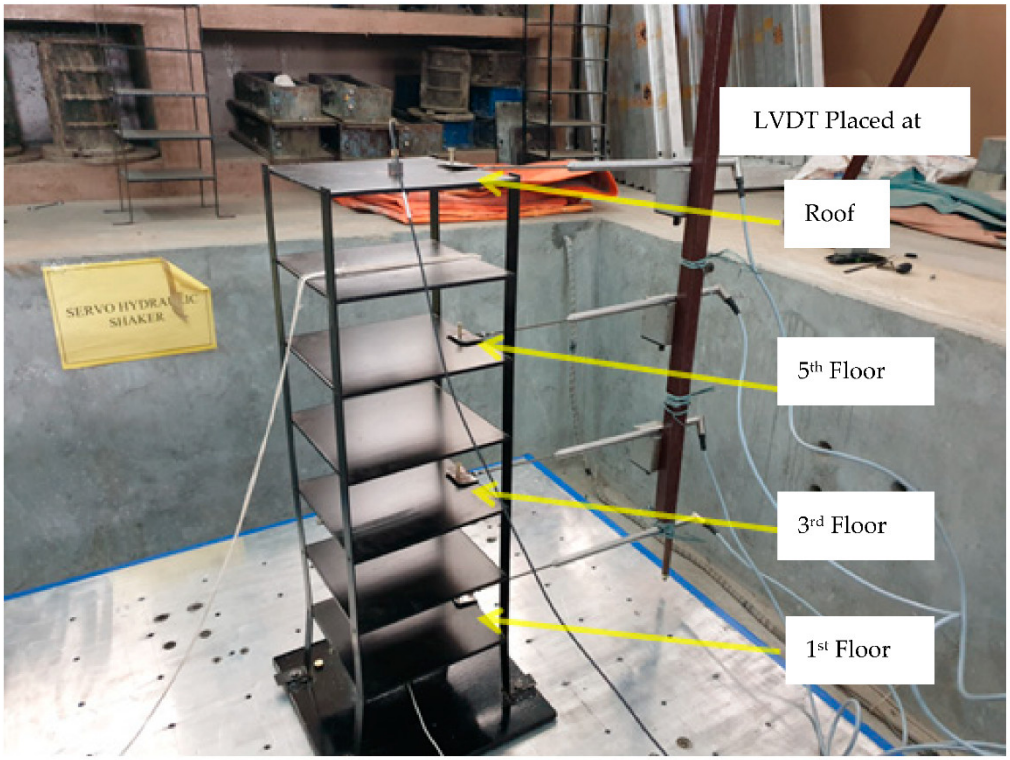

Figure 5. Shake-table test for the fixed-base structure.

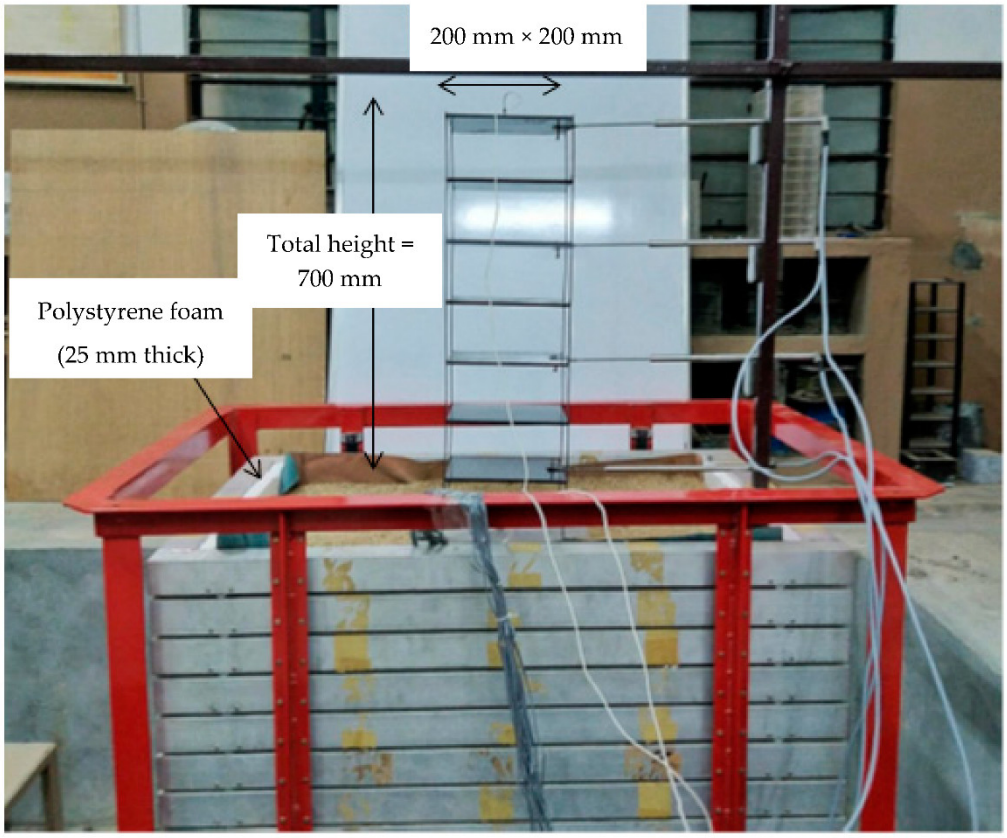

Figure 6. Shake table test for the soil-pile-supported structure, using the laminar shear box.

5. Free Vibration Analyses of the Structures

The natural time period (T) or fundamental natural frequency (f) plays a vital role in altering the spectral acceleration of the building. Moreover, the time period of a building with a flexible base increases as the flexibility of the soil-foundation system increases. This also modifies the energy dissipation capacity (i.e., damping) of the overall system. Hence, it is important to estimate the natural time period (or natural frequency) and damping of the soil-foundation-superstructure system.

The natural frequency of the system can be determined using free-vibration analysis. Any system that starts vibrating after it is subjected to an initial disturbance without any external force is considered to show free vibration. The natural frequency (f) and damping coefficient are the response parameters obtained from the free vibration of the damped system. The natural frequency (f) is dependent on mass (m) and stiffness (k). The unit for 'f' is hertz (Hz) or cycles per second (*cps*).

In a dynamic structural analysis, the damping forces are considered to be proportional to the amount of velocity [97]. This type of damping is known as viscous damping and is denoted by 'c'. The damping coefficient (ξ) of the system can be estimated using the commonly used approach known as the logarithmic decrement method. The symbol 'δ' denotes the logarithmic decrement. The degrading of the motion can be expressed as a logarithmic decrement from the time-history plot of the free vibration analysis. The time-history amplitude may be that of either acceleration or displacement. In this study, the displacement time history is used to compute the damping coefficient. This value is proportional to the logarithmic decrement. The damping of the system during free vibration is estimated using Equations (2) and (3) [97,98], as follows:

$$\xi = \frac{1}{2\pi}\delta \tag{2}$$

$$\xi = \frac{1}{2\pi} \ln \frac{X_1}{X_2} \quad (3)$$

where X_1 is the displacement at the first peak and X_2 is the displacement at the second peak.

In the free vibration test, a rope was tied to the roof of the model superstructure. The vibration was started using an initial displacement, applied by pulling on the rope. The displacement response of the model was recorded using the LVDT attached to the roof. First, the test was performed for each structural model by mounting it on the shake table. Second, the models with 3 × 3 piles made according to various slenderness ratios and spacings were placed in the soil, then the excitation results were captured. The tests were repeated three times for each model and the average frequency was estimated. For instance, the natural frequencies of the fixed-base model were measured for the three trials as 3.3, 3.04, and 3.24 Hz, respectively. Therefore, the natural frequency of the rigid-base structure was ascertained to be 3.22 Hz, which agrees closely with the calculated natural frequency of 3.10 Hz. The recorded displacement time history plot of the fixed-base and soil-pile-supported structures are shown in Figure 7a,b, respectively. The plots clearly display the decay of the motion.

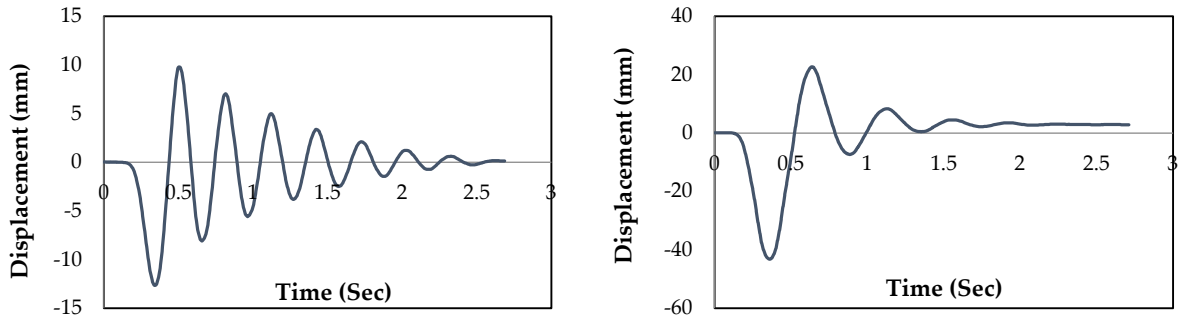

Figure 7. The free vibration displacement response of: (**a**) the fixed-base structure, and (**b**) the soil-pile-supported model (L = 15D and S = 3D).

The values of the natural frequency and damping ratio of the rigid-base and soil-pile-supported models were computed from these results and are presented in Figure 7.

In Figure 8, it is shown that the natural frequencies of the soil-pile-supported structures were lower than those of the rigid-base structures. The values corresponding to the soil-pile-supported models also increased as the spacing (from 3D to 9D) and the length of the pile foundations (from 15D to 60D) increased. A similar trend in frequency response was obtained by the authors of [99], by increasing the slenderness ratio of the piles. The main reason for this inference is that an increase in the spacing and slenderness ratio of the piles makes the overall system more rigid. A reduction of 16% in the natural frequency of the SPSI models with a pile slenderness ratio of 15D was obtained, compared to that with a pile slenderness ratio of 60D. Similarly, an increase in pile spacing from 3D to 9D increased the natural frequency by 21%.

Moreover, the damping ratio of the rigid-base and soil-pile-supported structures for varying pile group configurations was estimated. The damping ratio computed for a rigid-base building model was 5.3%, which is very close to the value (5%) that was suggested by [66] for the design of superstructures. It can be seen from Figure 8 that the soil-pile-supported models experienced higher damping ratio values compared to the rigid-base model. The damping of the flexible-base model decreased as the natural frequency of the same models increased. This trend is similar to the damping response obtained by the authors of [100] on soil-pile structure interaction studies. An increase in the damping ratio of 92% for the SPSI models concerning a pile with a length of 15D was attained when compared to that with a pile the length of 60D. Similarly, the increase in pile spacing from 3D to 9D decreased the damping by 56%.

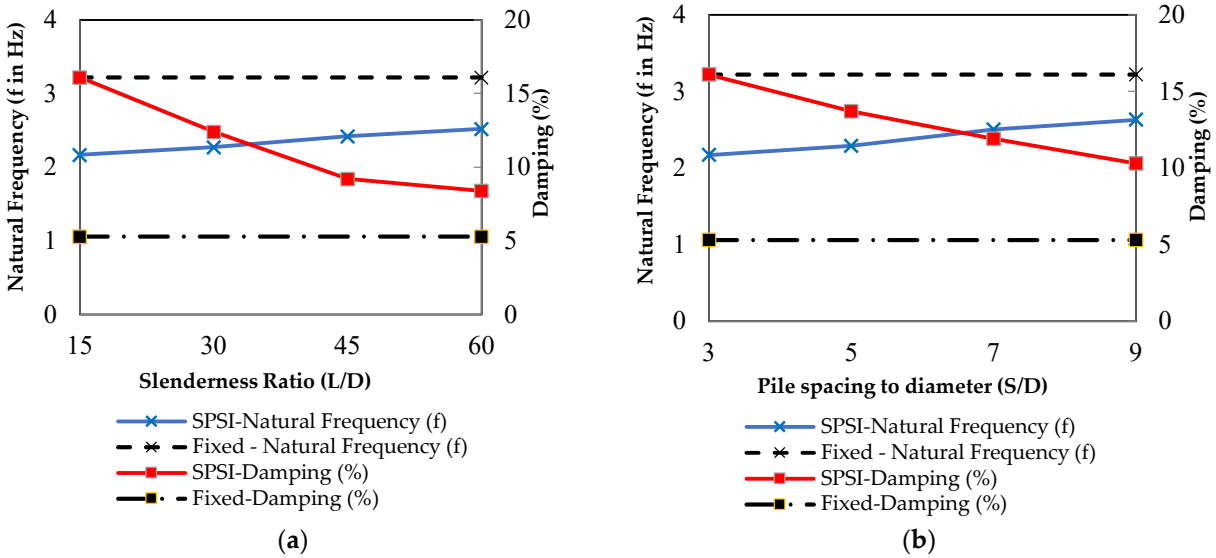

Figure 8. Comparison of the natural frequency and damping of an SPSI system and fixed-base structure: (**a**) a varying slenderness ratio for the models with S/D = 3, and (**b**) the varying spacing of piles for the models, with L/D = 15.

6. Forced Vibration of Structures

Seismic forces are used for the forced vibration analysis of fixed and flexible base-structure models. These earthquake forces can be applied in the form of either transient or periodic functions. Thus, in this study, earthquake forces are used in the way of periodic motion. In order to excite the shake table and to study the seismic response of the building model, parameters such as operating frequency, table acceleration, and displacement are necessary. The table acceleration (i.e., ground acceleration) can be estimated from the spectral acceleration of the superstructure. According to the authors of [66], the spectral acceleration coefficient (S_a/g) can be calculated using the formula of $1.34/T$ for the building wherein the time period (T) lies between 0.55 and 4.00 s and the soil is medium-dense. The soil conditions considered for the design of the prototype superstructure and foundations were medium. Hence, a medium-dense sandy soil with a relative density of 50% was adopted for this study. The natural time period of the seven-story prototype superstructure of 28 m in height was obtained from the modal analysis, using SAP2000 as 2.04 s (0.49 Hz). The prototype building has a plan dimension of 8 m × 8 m. Therefore, the value of S_a/g was computed as 0.67, which can be multiplied with the zone factor to ascertain the peak ground acceleration (PGA) of the building. The building structure was assumed to be located in Vellore city, which has a seismic zone factor of 0.16. Thus, considering all these parameters, the spectral acceleration (S_a) of the superstructure and peak ground acceleration (PGA) were computed to be 0.67 g and 0.107 g, respectively. Therefore, in this study, the Bhuj (2001) earthquake acceleration time history, which has a moment magnitude (M_w) of 7.7 and a PGA of 0.104 g, was used for the forced vibration analysis. The time-history plot of the Bhuj ground motion is shown in Figure 9.

As the shake table has operating specifications in terms of displacement (X) and frequency (f) for harmonic vibration, the acceleration (a) and constant table displacement of 5 mm were used to find the operating frequency, using the formula from [98], $a = -(2\pi f)^2 X$. The value of the operating frequency of the rigid-base structure was ascertained to be 2.29 Hz. The building model was excited with an operating frequency of 2.29 Hz for a table displacement of 5 mm. The behavior of the superstructure, in terms of story lateral displacement, and pile foundations, in terms of strain measurements along the length, were obtained and discussed.

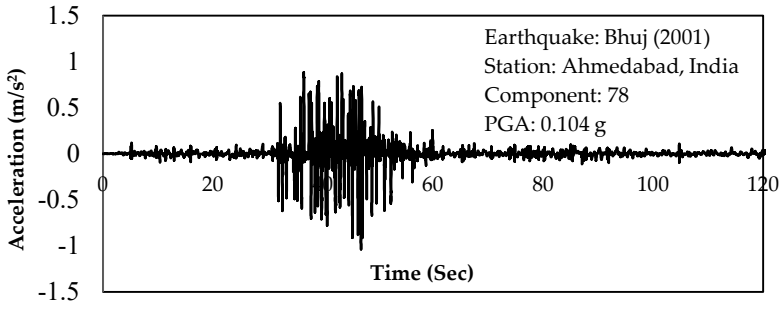

Figure 9. Bhuj (2001) acceleration time history.

6.1. Pile Bending Moment

The pile bending moment plays an important role in soil-pile-structure interaction, especially in the pile group. The bending moment profile of the pile along the length can be plotted by estimating the moment, using the measured strain values. The variation of strain measured along the length of the pile foundation over time is shown in Figure 10a,b. The bending moment can be computed using the simple/pure bending theory via Equation (4), as follows:

$$M = \frac{-E \times \varepsilon \times I}{y} \tag{4}$$

where M = bending moment; E = elastic modulus of the pile material; ε = measured strain; I = moment of inertia; y = distance from the neutral axis to the extreme fiber of the cross-section. The elastic modulus of the pile material (aluminum) is ascertained to be 70,000 MPa. The sample record of the strain measured in the pile foundation at the level of 0.21 L from the top is plotted in Figure 10a. It can be seen from Figure 10b that the maximum strain is measured at a level of 0.21 L from the top.

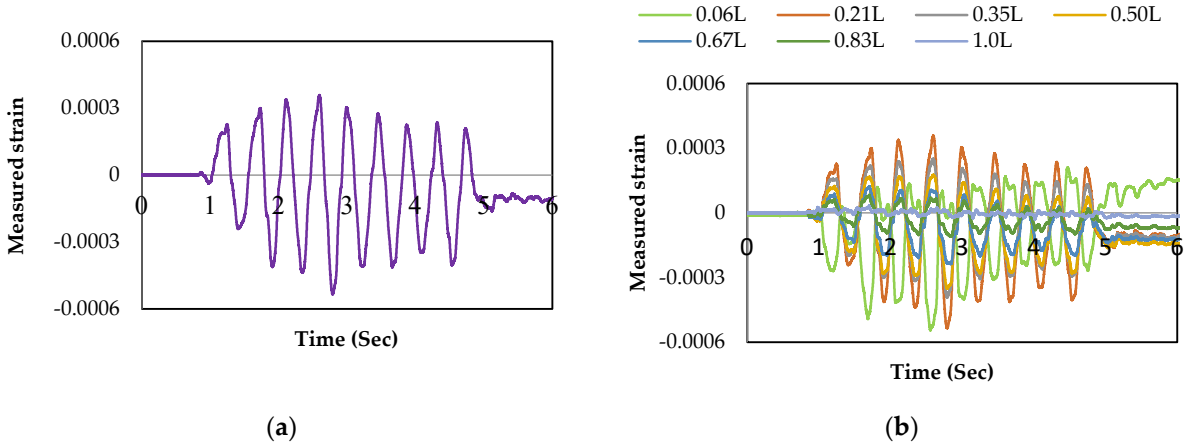

Figure 10. Typical strain measurements in the pile: (**a**) at the level of 0.21 L from the top (L = 60D and S = 3D), and (**b**) at all levels for the model, where L = 60D and S = 3D.

The estimated bending moment profile of the pile along its length for the front, middle, and rear row piles are plotted in Figure 11. This shows that the pile experienced the maximum bending moment at the level of 0.21 L from the top in the front and rear row piles. Similarly, the bending moment profile also remained the same. However, the middle-row pile attained the maximum value at the level of 0.35 L from the pile top. The maximum bending moment evaluated for the front, middle, and rear row piles are 882 N-mm, 822 N-mm, and 989 N-mm, respectively. This clearly demonstrates that the effect of pile-soil-pile interaction causes the stiffness degradation of soil and, consequently, increases the bending moment in the front and rear row piles.

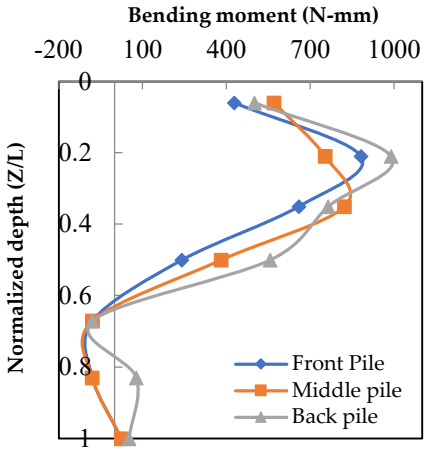

Figure 11. Bending moment profile of the piles for slenderness $L = 60D$ and spacing $S = 3D$.

Moreover, the effect of pile slenderness (L/D) on the bending moment values was investigated. The bending moment profile over the length of the pile for various lengths of 15D, 30D, 45D, and 60D for the pile-to-pile spacing of 3D is plotted in Figure 12a. The maximum value attained for the L/D = 15 is 495 N-mm at the level of 0.25 L from the top of the pile. It is clear from the bending moment profile plot for the slenderness ratio of L/D = 15 that the piles behave as a short rigid component. The bending moment of the piles also increased as the slenderness ratio increased. This response is similar to the dynamic bending moment profile reported by [90,99]. The maximum bending moment values computed for piles with slenderness ratios L/D = 30, 45, and 60 were 572 N-mm, 780 N-mm, and 881 N-mm, respectively. Thus, it can be inferred from the bending moment plots that the piles started behaving as flexible components when the slenderness ratio increased.

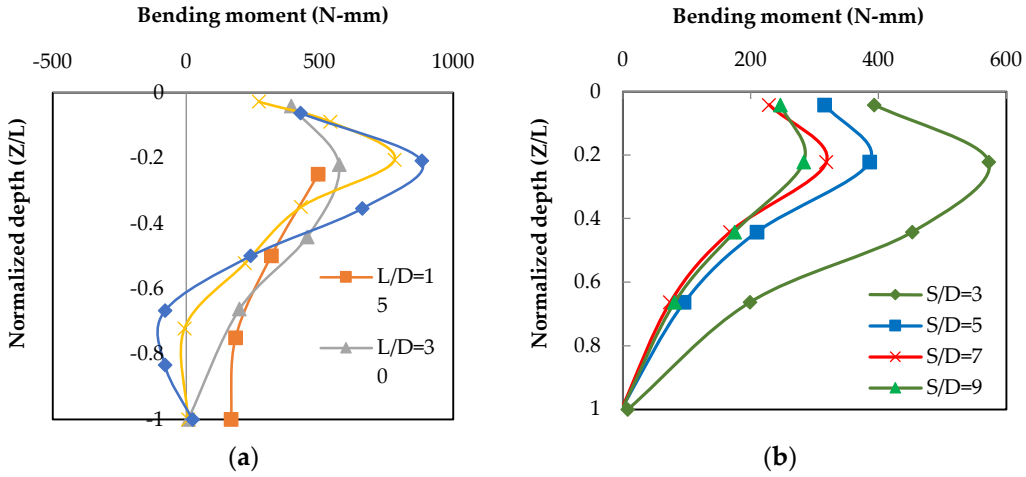

Figure 12. Bending moment profile: (**a**) effect of the slenderness of the pile for spacing $S = 3D$, and (**b**) effect of spacing of the piles for a slenderness value of $L = 30D$.

Furthermore, the bending moment profile over the pile length for various pile spacings, ranging from 3D *to* 9D, for a pile slenderness value of 30D, is plotted and is shown in Figure 12b. The highest value of the bending moment (573 N-mm) occurs at the piles modeled with a spacing of 3D, compared to other spacing piles. The maximum values estimated for the piles with spacings of 5D, 7D, and 9D are 386 N-mm, 318 N-mm, and 283 N-mm, respectively. It can be inferred from the bending moment profile plot for the scenarios of the various spacings that the piles experience higher values of bending moment as the spacing of the piles decreases. This is because of the group action of piles, which reduces the lateral resistance due to the degradation of soil stiffness. The reduction in soil stiffness makes the slender pile (L/D = 60) more flexible, with higher values of bending

moment. Although the pile failure depends on the flexural behavior in such a case, this may result in larger inelastic deformation due to the development of second-order bending moments. A similar type of response is observed in the failure of a bridge resting on pile foundations during the 1964 Niigata earthquake [18]. In summary, the bending moment value of piles with an L/D = 60 attains a 78% higher value than that of piles with L/D = 15. The bending moment values of closely spaced piles with S/D = 3 reach values 102% higher than those of the large spacing piles with S/D = 9D.

6.2. Story Lateral Displacement

Soil-pile-structure interaction may significantly amplify the lateral story displacements of buildings, especially in those resting on soft soils and with closely spaced pile foundations. Thus, a parametric study was conducted to evaluate the seismic behavior of rigid-base and flexible-base building frames. The seismic response parameter of the superstructure, in terms of story lateral displacement (X) was chosen and estimated. The sample records of the displacement time history obtained at the roof level and other floor levels of the rigid-base superstructure are shown in Figure 13a,b, respectively.

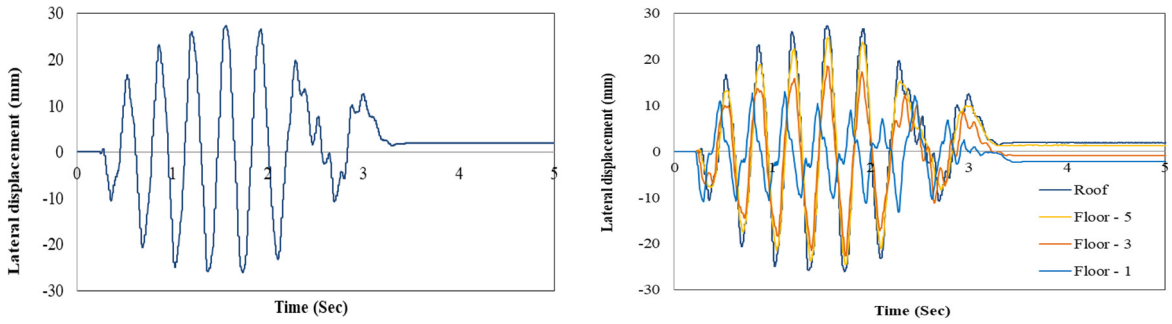

Figure 13. Typical experimental time-history displacement results of the fixed-base structure: (**a**) only at roof level, and (**b**) comparison of the displacements with other floors.

The profile of the maximum story lateral displacement of rigid-base and soil-pile-supported superstructures resting on shorter piles (L = 15D) over story levels is plotted and shown in Figure 14a. The plot shows that the soil-pile-supported structures attained higher values of story lateral displacement than in the rigid-base structure. It is obvious that the decrease in the natural frequency of the flexible-base models caused an increase in story displacement. Moreover, the displacement values are high in the case of structures resting on 3D-spaced pile foundations. The maximum story displacement of 36.5 mm was obtained for the 3D-spaced pile-supported structural models. The results clearly reveal that the lateral resistance offered by closely spaced (3D) pile foundations is reduced due to the degradation of soil stiffness because of group interaction effects. In addition, the story lateral displacement values of soil-pile-supported structures (X_{SPSI}) were normalized with rigid-base values (X_{RB}); the plot is shown in Figure 14b. It can be seen that the ratio of the story response parameter increased gradually from the top to the ground story level. The maximum normalized ratio of X_{SPSI}/X_{RB} value was computed for all structural models. The results reveal that the maximum X_{SPSI}/X_{RB} value of 3.48 was attained in closely spaced pile-supported models.

Similar to the impact of pile spacing on the seismic behavior of flexible-base structural models, the effect of pile slenderness was also studied. The plot of the maximum story displacement of rigid-base and flexible-base structures, supported on closely spaced pile foundations (3D), according to story level is shown in Figure 15a. The story displacement of a flexible-base structure supported on piles of varying slenderness, such as 15D, 30D, 45D, and 60D, was obtained and compared with the rigid-base model. It is clear that the structure resting on flexible piles (60D) experienced higher values of story displacements,

with a maximum of 40.3 mm at the roof. The variation of X_{SPSI}/X_{RB} values over story level was also plotted and is shown in Figure 15b. As expected, the higher values were observed for longer pile-supported structural models, with a maximum of 4.38 at the lower stories. The results obtained for story displacement and the X_{SPSI}/X_{RB} values of soil-pile-supported structures exhibit a similar trend, as observed in the numerical results presented in a previous paper [101]. From the reported findings, it is clear that pile group configuration has a considerable influence on structural story displacement. However, the impact of the pile slenderness ratio on story displacement was less than that of the spacing of piles for the same response parameter. In summary, the building models resting on piles of L/D = 60 attained 26% more lateral story displacement than those resting on piles of L/D = 15. Similarly, the models resting on closely spaced piles (3D) experienced 180% more lateral displacement than those resting on widely spaced piles (9D).

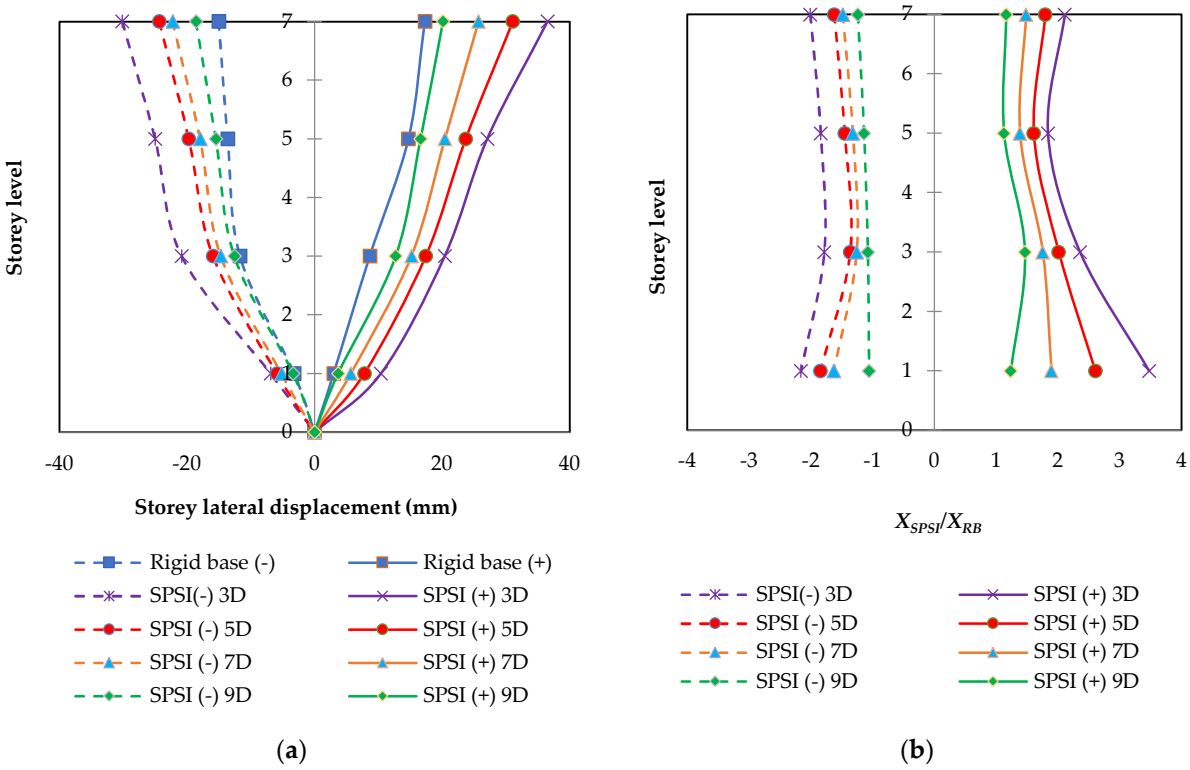

Figure 14. Effect of the S/D ratio on (**a**) story lateral displacement, and (**b**) X_{SPSI}/X_{RB} of the soil-pile-supported structural models, compared to the rigid-base structural model.

6.3. Inter-Story Drift

The inter-story drift ratio (*IDR*) is the dimensionless value that characterizes the lateral displacement of the story levels, with respect to the corresponding story height. This is the ratio of the difference between the lateral displacements of two adjacent story levels, according to the corresponding story height.

According to previous studies [102,103], the permissible value of *IDR* of the superstructure is 4% for the collapse level performance. Similarly, for the life safety level performance of the structure, the same value is limited to 1.5%. However, IS 1893 [66] recommends a permissible value of 0.4% for the elastic design of building frames. Various researchers [23,60,61] have conducted experimental works on the effect of SPSI on the earthquake response of buildings resting on clay. It was found that superstructures supported by pile foundations experienced higher *IDR* values compared to rigid-base models. However, the *IDR* values of most of the models exceeded the life safety performance level. Similar to the previous studies, the *IDR* values of a superstructure resting on friction pile foundations surrounded by sandy soil are quantified in the present study. The effects of the spacing

and length of pile foundations on the *IDR* values of rigid- and flexible-base buildings are estimated and compared.

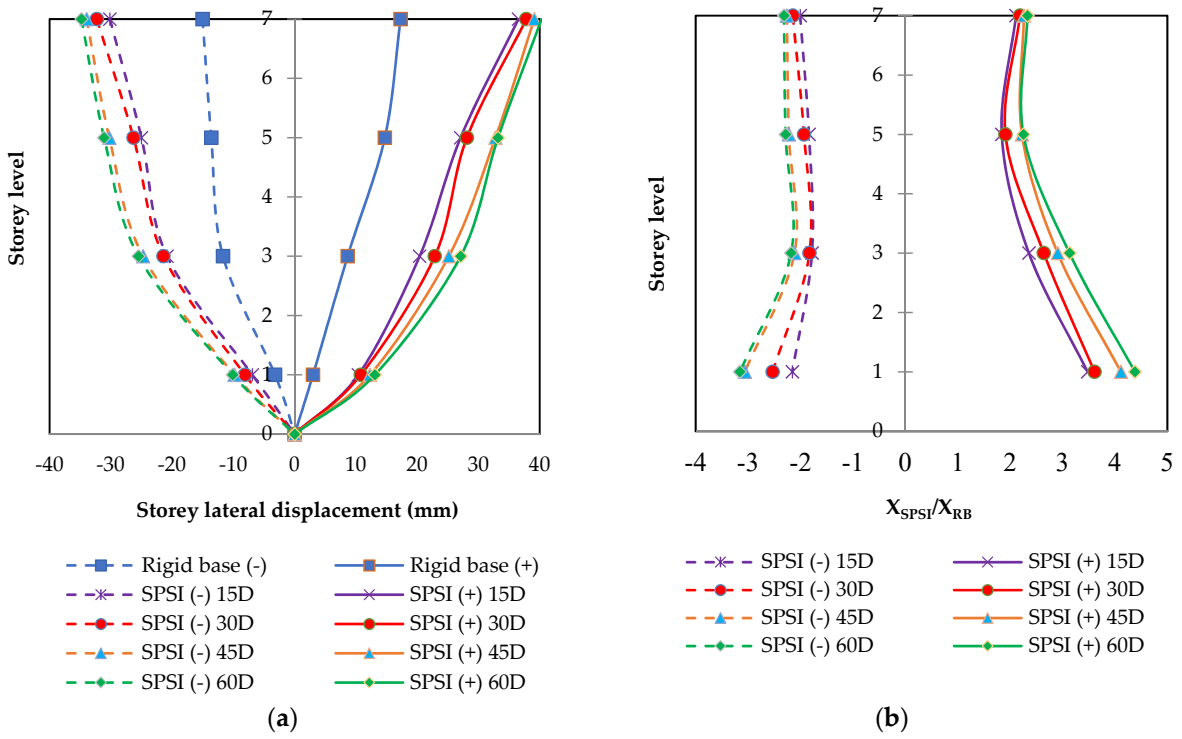

Figure 15. Effect of the *L*/*D* ratio on: (**a**) story lateral displacement, and (**b**) the X_{SPSI}/X_{RB} of the soil-pile-supported structural models, compared to the rigid-base structural model.

The prototype building, which has a natural frequency of 0.49 Hz, was designed for an elastic limit of 0.4% inter-story drift. However, the values of IDR increased to a maximum of 7%, which is far more than the permissible limit of 4%, corresponding to the collapse state performance level, as per FEMA373 [102]. This is because the building becomes more flexible, due to the effects of SPSI. Moreover, it can be seen from Figures 16 and 17 that the IDR corresponding to the fixed base is within the collapse level. Although the rigid-base building exceeded the life safety performance level, the collapse of the building is prevented. However, the IDR corresponding to flexible-base models exceeded the collapse state performance level. The story lateral displacement of the building is the sum of ground displacement (table displacement), the rocking component of the pile cap, and the rotational component of the superstructure. The difference in the uniformity of the IDR profile in both the left and right sides may be due to the effects of the rocking component of the pile cap. The non-uniform rocking of the foundation (pile cap) modified the overall lateral displacement of the superstructure models. In addition, the story displacement of the rigid-base and SPSI models agrees well with the response obtained by the other researchers [62].

The *IDR* values of soil-pile-supported structures are higher than the fixed base and exceeded the maximum permissible value of 4% given by [102,103]. The profile of *IDR* values of fixed-base and soil-pile-supported structures resting on shorter pile foundations ($L = 15D$) over story levels of varying spacing to diameter ratio (S/D) is shown in Figure 16a. The structures supported by closely spaced pile foundations ($3D$) attained maximum *IDR* values of 7% at 1/3 of the building height. Similarly, the ratios of *IDR* values of flexible-base structures for the varying S/D ratios to the *IDR* values of the rigid-base structure were estimated, and the profile is plotted in Figure 15b for the varying spacing of piles. The maximum normalized ratio IDR_{SPSI}/IDR_{RB} values are observed in the upper and lower story levels. The structure with $3D$ spacing piles experienced a higher normalized ratio

IDR_{SPSI}/IDR_{RB}, with a value of 3.67 at the upper story level. The results clearly illustrate the effects of the spacing of piles on superstructure performance levels.

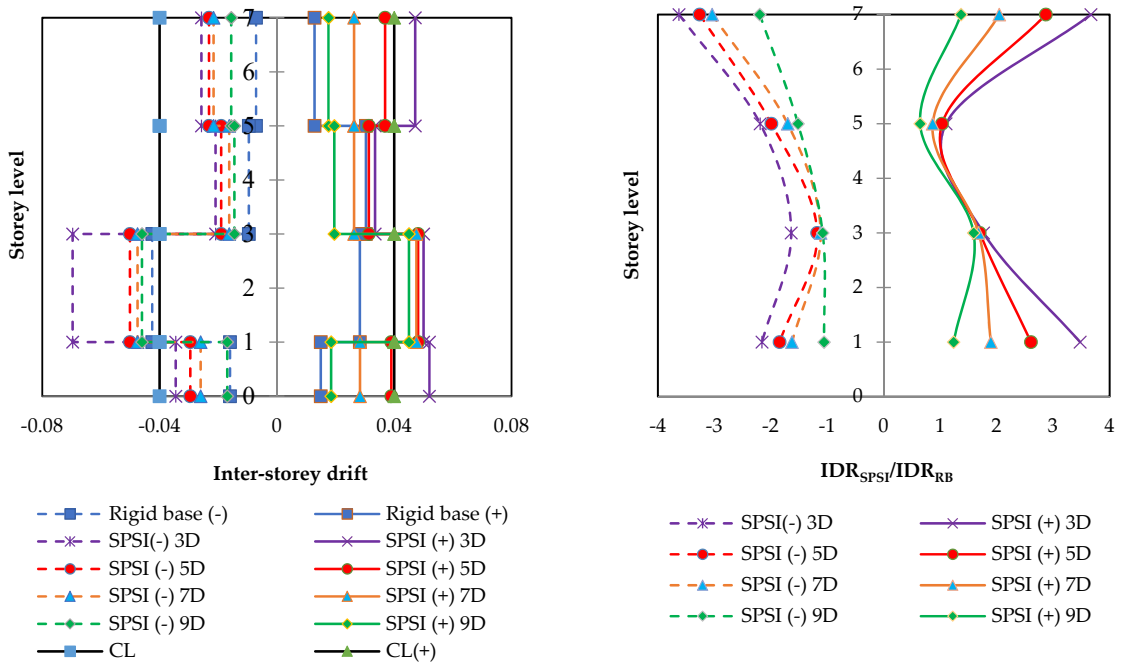

(**a**) (**b**)

Figure 16. Effect of *S/D* ratio on (**a**) inter-story drift ratio and (**b**) IDR_{SPSI}/IDR_{RB} of soil-pile-supported structural models compared to a rigid-base structural model.

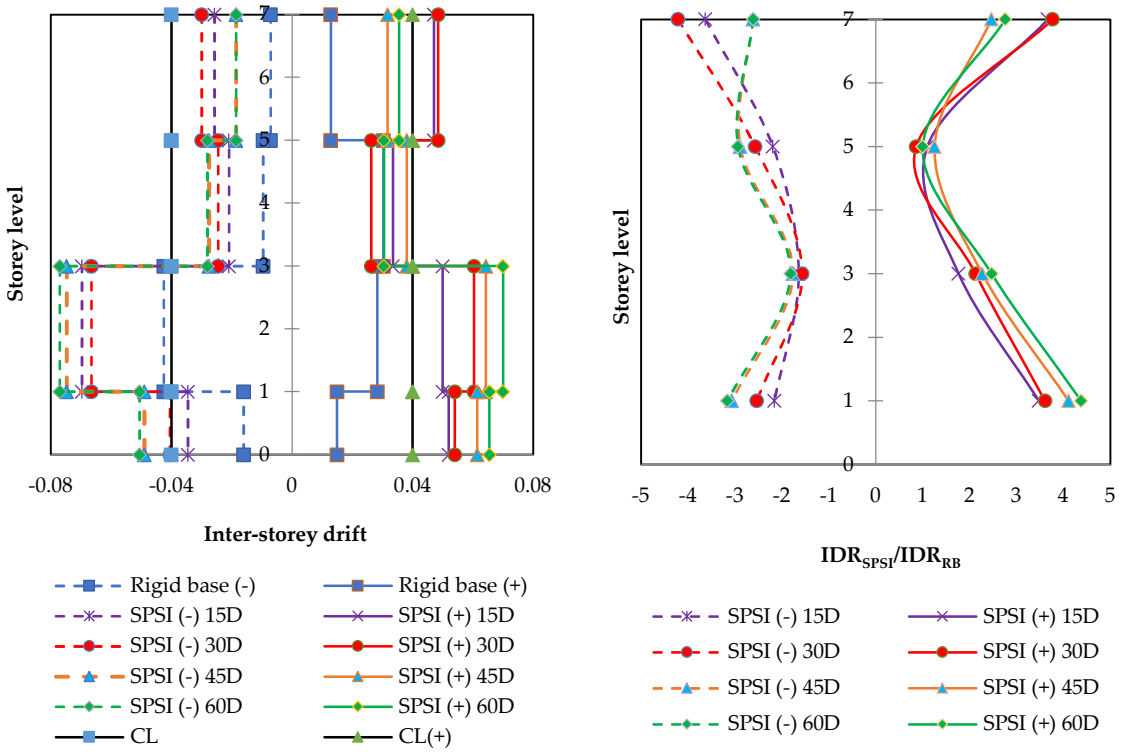

(**a**) (**b**)

Figure 17. Effect of the *L/D* ratio on (**a**) the inter-story drift ratio and (**b**) IDR_{SPSI}/IDR_{RB} of soil-pile-supported structural models, compared to a fixed-base structure.

The variation of the profile of *IDR* values of the fixed-base and soil-pile-supported structures resting on closely spaced pile foundations (S = 3D) over story levels is shown in Figure 17a. The structures supported by longer pile foundations (L = 60D) attained maximum IDR values of 7.7% at 1/3 of the building height. Similarly, the ratios of the *IDR* values of flexible-base structures for the varying L/D ratios to the *IDR* values of the rigid-base structure are estimated, and the relevant graph is shown in Figure 17b. The model with a 60D length of pile foundations experienced a higher normalized ratio IDR_{SPSI}/IDR_{RB} with a value of 4.21 at the upper-story level. The results clearly illustrate the effects of the slenderness ratio of pile foundations on superstructure performance levels. Although both the pile-design parameters (spacing and slenderness ratio) have considerable influence on the *IDR* values of the superstructure, the pile spacing effect is significant.

Based on the results, the building models resting on slender piles with L/D = 60 experienced 46% more inter-story drift values than those of the models resting on short rigid piles, with L/D = 15. Similarly, the models resting on closely spaced piles (3D) attained 167% more inter-story drift values than in the models resting on widely spaced piles (9D).

7. Discussion

The main purpose of this study is to quantify the effects of soil-pile-structure interaction on the seismic behavior of buildings resting on sand. An experimental study using a shake table was performed on rigid-base and flexible-base seven-story scaled building models. With a flexible base, the building models were resting on a pile foundation embedded in sandy soil, with a relative density of 50%. The pile foundations were designed for a 3 × 3 group with a pile cap. A parametric study on the varying pile spacing (3D, 5D, 7D, and 9D) and varying slenderness ratios of the piles (15, 30, 45, and 60) was carried out. As the spectral acceleration of the superstructure building depends on time period, the type of soil, and damping, a free vibration analysis was performed. The results of natural frequency and damping were computed and discussed. Since the natural frequency and damping values vary considerably due to the effects of pile spacing and pile length, proper care must be taken during the analysis and design of a superstructure. Otherwise, the behavior of the structure becomes affected detrimentally when the modified natural frequency of the system (due to the effects of SPSI) matches with the dominant frequency of the ground motion. In addition, the damping values of the SPSI models increased heavily when compared to the rigid-base models. This is because of a system that becomes more flexible, considering the SPSI effects. It will thus increase the lateral displacement of the superstructure, which will ultimately result in unacceptable serviceability requirements.

Moreover, a forced vibration analysis in the form of periodic motion was conducted on both rigid-base and flexible-base models. The behavior of the pile foundations and superstructure was captured in the form of pile strain and story lateral displacements. Considering the type of pile as either rigid or flexible is one of the most significant parameters for the analysis and design of piles. However, such soil-foundation effects are ignored in terms of the overall response of the superstructure system during the design phase. The degradation of soil stiffness arises due to the group interaction effects occurring when the piles are designed to be closely spaced and slender. This makes the pile foundation more flexible and results in a higher bending moment. It also increases the pile's inelastic deformation, which finally amplifies the story's lateral displacement and inter-story drift of the superstructure. Therefore, proper consideration should be given to the soil-structure interaction effects during the analysis and design phases.

8. Conclusions

The results of experiments conducted on a rigid model and soil-pile-supported superstructures have been discussed. The effects of spacing and the slenderness of pile foundations on natural frequency, damping, pile bending moment, story lateral displacement, and inter-story drift ratio were illustrated. The effects of pile design parameters on the ratios of X_{SPSI}/X_{RB} and IDR_{SPSI}/IDR_{RB} were computed, and the results are reported

herein. Based on an experimental study of the seismic behavior of soil-pile-supported superstructure models, the following conclusions can be drawn.

1. The natural frequency values of the flexible-base models increased compared to the rigid-base models. The pile slenderness ratio and spacing have great effects on the natural frequency of the soil-pile-supported models. The natural frequency of SPSI models with a pile length of 15D was reduced by 16%, compared to those of the model with a pile length of 60D. Similarly, the increase in pile spacing from 3D to 9D increased the natural frequency by 21%.
2. Similarly, the damping values of the SPSI models decreased compared to those of the fixed-base models. The damping of the flexible-base models with a pile length of 15D increased by 92%, in comparison to that of the model with a pile length of 60D. The rigidity at the base of the model also increased when the spacing between the piles was large (S = 9D). This decreased the value of damping by 56% compared to that of the model with closely spaced piles (S = 3D). This increase in damping in shorter pile models may alter the inelastic deformation of the superstructure.
3. The pile bending moment due to the dynamic lateral loading increased by 78% for the model with L/D = 60, in comparison to that of the model with L/D = 15. This is due to the fact that the piles started behaving as flexible components when the slenderness ratio increased. Similarly, the group action of the piles reduced the lateral resistance due to the degradation of soil stiffness for closely spaced pile models. Therefore, we saw a rise in pile bending moment by 102% for the structure resting on closely spaced piles (3D), compared to that of the model with large spacing (9D).
4. The seismic response of the superstructure was significantly influenced by the behavior of the soil-foundation system. The higher value of story lateral displacement was attained with the model resting on closely spaced (S = 3D) slender piles (L = 60D). The corresponding ratio of story displacement of the SPSI model compared to the rigid-base model (X_{SPSI}/X_{RB}) was estimated to be 4.38. This demonstrates the significance of considering the soil-pile-structure interaction during the analysis and design stages.
5. Moreover, the increase in the slenderness ratio and decrease in pile spacing increased the story lateral displacement considerably. The value of the superstructure story lateral displacement increased by 26% for the model supported by piles of L/D = 60, compared to that of the model with piles of L/D = 15. Similarly, reducing the spacing of the piles to 3D increased the lateral story displacement by 180%. This is due to the increase in pile bending moment, the decrease in natural frequency, and the increase in the damping of the system.
6. Inter-story drift (*IDR*) is one of the most important design parameters for the limit state design of serviceability. The ratio of *IDR* values for the flexible base (model with S/D = 3 and L/D = 60) compared to the rigid base was computed to be 4.21. Furthermore, the model with the closely spaced piles (S/D = 3) experienced an *IDR* value of 167% more than that of the model with an S/D = 9. The increase in slenderness ratio to L/D = 60 also increased the *IDR* value by 46%, compared to that of the model with L/D = 15.
7. As an increase or decrease in natural frequency may alter the spectral acceleration and resulting base shear, it is important to consider the SPSI effects in the design parameters. Moreover, the spacing and slenderness ratio of piles play a vital role in the seismic behavior of building frames. The closely spaced slender pile group model becomes more flexible due to soil degradation and the flexural behavior of piles. Therefore, proper consideration must be given to the design parameters, such as the time period, damping, soil properties, and foundation details during the design process of superstructures. However, soil-pile-structure interaction effects should be incorporated in building design to eliminate the under/overestimation of the forces at work in the design.

The obtained results clearly illustrate the importance of soil-structure interaction during the analysis and design of foundations and buildings. Moreover, the pile slenderness ratio and pile spacing have considerable effects on the seismic behavior of the soil-foundation-superstructure system. This alters the overall response of the system significantly. In addition, the study can be extended by varying the design parameters, such as the soil relative density, soil type, layered soil deposits, the number of piles in the group, and the pile group arrangement.

Author Contributions: Conceptualization, J.A.V. and S.S.C.; methodology, J.A.V.; investigation, J.A.V.; resources, J.A.V.; writing—original draft preparation, J.A.V.; writing—review and editing, S.S.C.; supervision, S.S.C.; project administration, S.S.C. All authors have read and agreed to the published version of the manuscript.

Funding: This research received no external funding.

Data Availability Statement: All data have been provided in the corresponding chapters of the paper.

Acknowledgments: The authors would like to thank the Vellore Institute of Technology for providing materials and instruments and also for the use of its laboratory facilities.

Conflicts of Interest: The authors declare no conflict of interest.

Appendix A

Scaling Calculations:
Length:
Scaled model length = (1/n) × Prototype length
Where, n = 40
Width of prototype building—8m
Width of scaled model—8 m × (1/n) = 8000 × 1/40 = 200 mm

Length of prototype building—8 m
Length of scaled model—8 m × (1/n) = 8000 × 1/40 = 200 mm

Height of prototype building—28 m
Height of scaled model—28 m × (1/n) = 28,000 × 1/40 = 700 mm

Storey Height of prototype building—4 m
Storey Height of scaled model—4 m × (1/n) = 4000 × 1/40 = 100 mm

Volume:
Volume of scaled model = Volume of prototype × $(1/n^3)$
Volume of prototype = 8 m × 8 m × 28 m = 1792 m^3.
Therefore, volume of scaled model = $1792/40^3$ = 0.028 m^3 (0.2 × 0.2 × 0.7)

Stiffness:
Stiffness of the column of scaled model = Stiffness of the column of prototype × $(1/n^2)$
Stiffness of the prototype column = $12EI/L^3$
Where, E = Elastic modulus of concrete = 25,000 MPa
I = Moment of Inertia = $BD^3/12 = 500 \times 500^3/12 = 5.21 \times 10^9$ mm^4
L = 4000 mm
Stiffness of the one prototype column = 24,422 N-mm
Total stiffness of the storey = 9 × 24,422 = 219,797 N-mm
Therefore, stiffness of one scaled model = 219,797/4 = 54,949 N–mm = 54,949 × $(1/40^2)$ = 34.33 N-mm
Thus, dimension of scaled model column = $12EI/L^3$ = 34.33
E = Elastic modulus of steel = 2×10^5 N/mm^2.
L = 100 mm
I = $bt^3/12$
Thickness of column = 2 mm

Therefore, required width of column, $12EI/L3 = 12 \times 2 \times 10^5 \times b \times (2^3/12)/100^3 = 34.33$
So, b = 21.46 = 22 mm.
Adopt, 22 mm × 2 mm size column for scaled model.

Density:
Scaled model = 1 × Prototype
Density of prototype = Weight of the building/volume = 9048 kN/(8 m × 8 m × 28 m) = 5.05 kN/m^3 = 515 kg/m^3.
Therefore, required weight of scaled model = Density × volume = 515 × (0.2 × 0.2 × 0.7) = 14.4 kg.

Moreover, adopt 6 mm thickness slab for all storeys.
Total weight of the fabricated scaled model = Column weight + slab weight

Where, column weight	= No. of column × L × B × t × density = 4 × 0.7 (m) × 0.022 (m) × 0.002 (m) × 7850 kg/m^3 = 0.97 kg
Slab weight	= No. of slabs × B × L × t × 7850 = 7 × 0.2 × 0.2 × 0.006 × 7850 = 13.2 kg

Total weight of the scaled model = 0.97 + 13.2 = 14.17 kg, which is nearer to the required weight (14.4 kg).

Frequency:
Frequency of prototype = 0.49 Hz
Frequency of fixed base scaled model = 0.49 Hz × Scale factor ($n^{1/2}$) = 0.49 × $40^{0.5}$ = 3.10 Hz

References

1. Boominathan, A.; Ayothiraman, R. Dynamic behaviour of laterally loaded model piles in clay. *Proc. Inst. Civ. Eng. Geotech. Eng.* **2005**, *158*, 207–215. [CrossRef]
2. Boominathan, A.; Ayothiraman, R. An experimental study on static and dynamic bending behaviour of piles in soft clay. *Geotech. Geol. Eng.* **2007**, *25*, 177–189. [CrossRef]
3. Poulos, H.G.; Davis, E.H. *Pile Foundation Analysis and Design*; John Wiley and Sons: Chichester, UK, 1980.
4. Reese, L.C.; Isenhower, W.M.; Wang, S.T. *Analysis and Design of Shallow and Deep Foundations*, 1st ed.; Wiley: New York, NY, USA, 2005. [CrossRef]
5. Chandrasekaran, S.S.; Boominathan, A.; Dodagoudar, G.R. Group Interaction Effects on Laterally Loaded Piles in Clay. *J. Geotech. Geoenviron. Eng.* **2010**, *136*, 573–582. [CrossRef]
6. Brown, D.A.; Lymon, C.R.; O'Neill, M.W. Cyclic Lateral Loading of a Large-Scale Pile Group. *J. Geotech. Eng.* **1987**, *113*, 1326–1343. [CrossRef]
7. Rollins, K.M.; Peterson, K.T.; Weaver, T.J. Lateral Load Behavior of Full-Scale Pile Group in Clay. *J. Geotech. Geoenviron. Eng.* **1998**, *124*, 468–478. [CrossRef]
8. Fayez, A.F.; El Naggar, M.H.; Cerato, A.B.; Elgamal, A. Correction to: Assessment of SSI Effects on Stiffness of Single and Grouped Helical Piles in Dry Sand from Large Shake Table Tests. *Bull. Earthq. Eng.* **2022**, *20*, 3619. [CrossRef]
9. Wolf, J.P. *Dynamic Soil-Structure Interaction*; Prentice-Hall Inc.: Englewood Cliffs, NJ, USA, 1985.
10. Mylonakis, G.; Gazetas, G. Seismic soil-structure interaction: Beneficial or detrimental? *J. Earthq. Eng.* **2000**, *4*, 277–301. [CrossRef]
11. Somerville, P.G. The amplitude and duration effects of rupture directivity in near fault ground motions. In *Geotechnical Earthquake Engineering and Soil Dynamics III*; Dakoulas, P., Yegian, M.K., Holtz, R.D., Eds.; ASCE: Reston, VA, USA, 1998.
12. Gazetas, G.; Mylonakis, G. 'Seismic Soil-Structure Interaction: New evidence and emerging issues'. In *Geotechnical Earthquake Engineering and Soil Dynamics III*; Dakoulas, P., Yegian, M.K., Holtz, R.D., Eds.; ASCE: Reston, VA, USA, 1998; Volume 2, pp. 1119–1174.
13. Veletsos, A.S.; Meek, J.W. Dynamic behaviour of building-foundation systems. *Earthq. Eng. Struct. Dyn.* **1974**, *3*, 121–138. [CrossRef]
14. Tabatabaiefar, H.R.; Massumi, A. A simplified method to determine seismic responses of reinforced concrete moment resisting building frames under influence of soil–structure interaction. *Soil Dyn. Earthq. Eng.* **2010**, *30*, 1259–1267. [CrossRef]
15. Horii, K. *General Report on the Niigata Earthquake*; Part 3: Highway Bridges; Tokyo Electrical Engineering College Press: Tokyo, Japan, 1968; pp. 431–450.
16. Towhata, I. Photographs and Motion Picture of the Niigata City Immediately after the 1964 earthquake (CD). *Jpn. Geotech. Soc.* **1999**, *17*.

17. Kerciku, A.A.; Bhattacharya, S.; Lubkowski, Z.A.; Burd, H.J. Failure of Showa Bridge during the 1964 Niigatta Earthquake. In Proceedings of the 14th World Conference on Earthquake Engineering, Beijing, China, 12–17 October 2008.
18. Dash, S.R.; Bhattacharya, S. Mechanism of failure of three pile-supported structures during three different earthquakes. In Proceedings of the 15th World Conference on Earthquake Engineering, Lisboa, Portugal, 24–28 September 2012.
19. Meymand, P.J. Shaking Table Scale Model Tests of Nonlinear Soil-Pile-Superstructure Interaction in Soft Clay. Ph.D. Thesis, University of California Berkeley, Berkeley, CA, USA, 1998.
20. Mylonakis, G.; Gazetas, G.; Nikolaou, S.; Michaelides, O. The role of soil on the collapse of 18 piers of the Hanshin Expressway in the Kobe earthquake. In Proceedings of the 12th World Conference on Earthquake Engineering, Auckland, New Zealand, 30 January–4 February 2000.
21. Dash, S.R.; Govindaraju, L.; Bhattacharya, S. A case study of damages of the Kandla Port and Customs Office tower supported on a mat–pile foundation in liquefied soils under the 2001 Bhuj earthquake. *Soil Dyn. Earthq. Eng.* **2009**, *29*, 333–346. [CrossRef]
22. Smyrou, E.; Tasiopoulou, P.; Bal, I.E.; Gazetas, G. Ground Motions versus Geotechnical and Structural Damage in the February 2011 Christchurch Earthquake. *Seism. Res. Lett.* **2011**, *82*, 882–892. [CrossRef]
23. Hokmabadi, A.S.; Fatahi, B.; Samali, B. Assessment of soil–pile–structure interaction influencing seismic response of mid-rise buildings sitting on floating pile foundations. *Comput. Geotech.* **2014**, *55*, 172–186. [CrossRef]
24. Hokmabadi, A.S.; Fatahi, B. Influence of Foundation Type on Seismic Performance of Buildings Considering Soil–Structure Interaction. *Int. J. Struct. Stab. Dyn.* **2016**, *16*, 1550043. [CrossRef]
25. Van Nguyen, Q.; Fatahi, B.; Hokmabadi, A.S. Influence of Size and Load-Bearing Mechanism of Piles on Seismic Performance of Buildings Considering Soil–Pile–Structure Interaction. *Int. J. Géoméch.* **2017**, *17*, 04017007. [CrossRef]
26. Askouni, P.K.; Karabalis, D.L. The Modification of the Estimated Seismic Behaviour of R/C Low-Rise Buildings Due to SSI. *Buildings* **2022**, *12*, 975. [CrossRef]
27. Mori, F.; Mendicelli, A.; Moscatelli, M.; Romagnoli, G.; Peronace, E.; Naso, G. A new Vs30 map for Italy based on the seismic microzonation dataset. *Eng. Geol.* **2020**, *275*, 105745. [CrossRef]
28. Ruggieri, S.; Calò, M.; Cardellicchio, A.; Uva, G. Analytical-mechanical based framework for seismic overall fragility analysis of existing RC buildings in town compartments. *Bull. Earthq. Eng.* **2022**, 1–38. [CrossRef]
29. Alizadeh, M.; Davisson, M.T. Lateral Load Tests on Piles-Arkansas River Project. *J. Soil Mech. Found. Div.* **1970**, *96*, 1583–1604. [CrossRef]
30. Matlock, H. Correlations for design of laterally loaded piles in soft clay. In Proceedings of the 2nd Annual Offshore Technology Conference 1, Houston, TX, USA, 21 April 1970; Volume 1204, pp. 577–594.
31. Reese, L.C.; Cox, W.R.; Coop, F.D. Field testing and Analysis of laterally loaded piles in stiff clay. In Proceedings of the VII Annual Offshore Technology Conference, Houston, TX, USA, 4 May 1975; Volume 2, pp. 672–690.
32. Reese, L.C.; Welch, R.C. Lateral Loading of Deep Foundations in Stiff Clay. *J. Geotech. Eng. Div.* **1975**, *101*, 633–649. [CrossRef]
33. Kim, J.B.; Brungraber, R.J. Full-Scale Lateral Load Tests of Pile Groups. *J. Geotech. Eng. Div.* **1976**, *102*, 87–105. [CrossRef]
34. Ruesta, P.F.; Townsend, F.C. Evaluation of Laterally Loaded Pile Group at Roosevelt Bridge. *J. Geotech. Geoenviron. Eng.* **1997**, *123*, 1153–1161. [CrossRef]
35. Rollins, K.M.; Sparks, A. Lateral Resistance of Full-Scale Pile Cap with Gravel Backfill. *J. Geotech. Geoenviron. Eng.* **2002**, *128*, 711–723. [CrossRef]
36. Richards, P.W.; Rollins, K.M.; Stenlund, T.E. Experimental Testing of Pile-to-Cap Connections for Embedded Pipe Piles. *J. Bridg. Eng.* **2011**, *16*, 286–294. [CrossRef]
37. Franke, E. Principles for test loading of large bored piles by horizontal loads. In Proceedings of the 8th International Conference on Soil Mechanics and Foundation Engineering, Moscow, Russia, 6–11 August 1973; Volume 2, pp. 97–104.
38. Meimon, Y.; Baguelin, F.; Jezequel, J.F. Pile group behavior under long time lateral monotonic and cyclic loading. In Proceedings of the Third International conference on Numerical methods in Offshore Piling, Nantes, France, 21–22 May 1986; pp. 285–302.
39. Brown, D.A.; Clark, M.; Reese, L.C. Lateral Load Behavior of Pile Group in Sand. *J. Geotech. Eng.* **1988**, *114*, 1261–1276. [CrossRef]
40. Dunnavant, T.W.; Michael, W.O. Experimental P-y Model for Submerged, Stiff Clay. *J. Geotech. Eng.* **1989**, *115*, 95–114. [CrossRef]
41. Chai, Y.H.; Hutchinson, T.C. Flexural Strength and Ductility of Extended Pile-Shafts. II: Experimental Study. *J. Struct. Eng.* **2002**, *128*, 595–602. [CrossRef]
42. Rollins, K.M.; Olsen, K.G.; Jensen, D.H.; Garrett, B.H.; Olsen, R.J.; Egbert, J.J. Pile Spacing Effects on Lateral Pile Group Behavior: Analysis. *J. Geotech. Geoenviron. Eng.* **2006**, *132*, 1272–1283. [CrossRef]
43. Rollins, K.M.; Olsen, R.J.; Elbert, J.J.; Jensen, D.H.; Olsen, K.G.; Garrett, B.H. Pile Spacing Effects on Lateral Pile Group Behavior: Load Tests. *J. Geotech. Geoenviron. Eng.* **2006**, *132*, 1262–1271. [CrossRef]
44. Tuladhar, R.; Maki, T.; Mutsuyosi, H. Cyclic behavior of laterally loaded concrete piles embedded into cohesive soil. *Earthq. Eng. Struct. Dyn.* **2007**, *37*, 43–59. [CrossRef]
45. Ting, J.M. Full-Scale Cyclic Dynamic Lateral Pile Responses. *J. Geotech. Eng.* **1987**, *113*, 30–45. [CrossRef]
46. Blaney, G.W.; O'Neill, M.W. Procedures for Prediction of Dynamic Lateral Pile Group Response in Clay from Single Pile Tests. *Geotech. Test. J.* **1991**, *14*, 3. [CrossRef]
47. Blaney, G.W.; O'Neill, M.W. Dynamic Lateral Response of a Pile Group in Clay. *Geotech. Test. J.* **1989**, *12*, 22. [CrossRef]
48. Han, Y.; Vaziri, H. Dynamic response of pile groups under lateral loading. *Soil Dyn. Earthq. Eng.* **1992**, *11*, 87–99. [CrossRef]
49. Novak, M.F.; Grigg, R. Dynamic experiments with small pile foundations. *Can. Geotech. J.* **1976**, *13*, 372–385. [CrossRef]

50. El Shamouby, B.; Novak, M. Dynamic Experiments with Group of Piles. *J. Geotech. Eng.* **1984**, *110*, 719–737. [CrossRef]
51. Hassini, S.; Woods, R.D. Dynamic experiments with model pile foundations. In Proceedings of the 12th International Conference on Soil Mechanics and Geotechnical Engineering, Rio de Janeiro, Brazil, 2–15 September 1989; pp. 1135–1138.
52. El-Marsafawi, H.; Han, Y.C.; Novak, M. Dynamic Experiments on Two Pile Groups. *J. Geotech. Eng.* **1992**, *118*, 576–592. [CrossRef]
53. Burr, J.P.; Pender, M.J.; Lankin, T.J. Dynamic Response of Laterally Excited Pile Groups. *J. Geotech. Geoenviron. Eng.* **1997**, *123*, 1–8. [CrossRef]
54. Chau, K.T.; Shen, C.Y.; Guo, X. Nonlinear seismic soil–pile–structure interactions: Shaking table tests and FEM analyses. *Soil Dyn. Earthq. Eng.* **2009**, *29*, 300–310. [CrossRef]
55. Ishimura, K.; Ohtsuki, A.; Yokoyama, K.; Koyangi, Y. Sway rocking model for simulating nonlinear response of sandy deposit with structure. In Proceedings of the 10th World Conference on Earthquake Engineering, Madrid, Spain, 19–24 July 1992; pp. 1897–1903.
56. Pitilakis, D.; Dietz, M.; Wood, D.M.; Clouteau, D.; Modaressi, A. Numerical simulation of dynamic soil–structure interaction in shaking table testing. *Soil Dyn. Earthq. Eng.* **2008**, *28*, 453–467. [CrossRef]
57. Pan, T.-C.; Goh, K.; Megawati, K. Empirical relationships between natural vibration period and height of buildings in Singapore. *Earthq. Eng. Struct. Dyn.* **2013**, *43*, 449–465. [CrossRef]
58. Ruggieri, S.; Andrea, F.; Uva, G. A New Approach to Predict the Fundamental Period of Vibration for Newly-designed Reinforced Concrete Buildings. *J. Earthq. Eng.* **2021**, *26*, 6943–6968. [CrossRef]
59. Hatzigeorgiou, G.D.; Kanapitsas, G. Evaluation of fundamental period of low-rise and mid-rise reinforced concrete buildings. *Earthq. Eng. Struct. Dyn.* **2013**, *42*, 1599–1616. [CrossRef]
60. Hokmabadi, A.S.; Fatahi, B.; Samali, B. Physical Modeling of Seismic Soil-Pile-Structure Interaction for Buildings on Soft Soils. *Int. J. Géoméch.* **2015**, *15*, 04014046. [CrossRef]
61. Tabatabaiefar, H.R.; Fatahi, B.; Ghabraie, K.; Zhou, W. Evaluation of numerical procedures to determine seismic response of structures under influence of soil-structure interaction. *Struct. Eng. Mech.* **2015**, *56*, 27–47. [CrossRef]
62. El Hoseny, M.; Ma, J.; Dawoud, W.; Forcellini, D. The role of soil structure interaction (SSI) on seismic response of tall buildings with variable embedded depths by experimental and numerical approaches. *Soil Dyn. Earthq. Eng.* **2023**, *164*, 107583. [CrossRef]
63. Patil, G.; Choudhury, D.; Mondal, A. Three-Dimensional Soil–Foundation–Superstructure Interaction Analysis of Nuclear Building Supported by Combined Piled–Raft System. *Int. J. Géoméch.* **2021**, *21*, 04021029. [CrossRef]
64. *IS 875-Part 1*; Code of Practice for Design Loads (Other Than Earthquake) for Buildings and Structures—Dead Loads—Unit Weights of Building Materials and Stored Materials. Reaffirmed (2018); Bureau of Indian Standards: New Delhi, India, 1987.
65. *IS 875-Part 2*; Code of Practice for Design Loads (Other Than Earthquake) for Buildings and Structures—Imposed Loads. Reaffirmed (2018); Bureau of Indian Standards: New Delhi, India, 1987.
66. *IS 1893-Part 1*; Criteria for Earthquake Resistant Design of Structures—General Provisions and Buildings. Bureau of Indian Standards: New Delhi, India, 2016.
67. *IS 456*; Plain and Reinforced Concrete—Code of Practice. Reaffirmed (2005); Bureau of Indian Standards: New Delhi, India, 2000.
68. *SAP2000*, Computer Software; Computers and Structures: California, CA, USA, 2019.
69. *IS 2720-Part 3*; Methods of Tests for Soils—Determination of Specific Gravity—Fine Grained Soils. Sec 1—Reaffirmed (2016); Bureau of Indian Standards: New Delhi, India, 1980.
70. *IS 2720-Part 14*; Determination of Density Index (Relative Density) of Cohesionless Soils. Reaffirmed (2020); Bureau of Indian Standards: New Delhi, India, 1983.
71. *IS 2720-Part 13*; Direct Shear Test. Reaffirmed (2016); Bureau of Indian Standards: New Delhi, India, 1986.
72. *IS 2720-Part 4*; Methods of Tests for Soils—Grain Size Analysis. Reaffirmed (2020); Bureau of Indian Standards: New Delhi, India, 1985.
73. *D2487-17*; Standard Practice for Classification of Soils for Engineering Purposes (Unified Soil Classification System). ASTM: West Conshohocken, PA, USA, 2020.
74. *IS 2911-Part 1/Sec 2*; Design and Construction of Pile Foundations—Code of Practice. Bureau of Indian Standards: New Delhi, India, 2010.
75. Wood, D.M.; Crewe, A.; Taylor, C. Shaking table testing of geotechnical models. *Int. J. Phys. Model. Geotech.* **2002**, *2*, 1–13. [CrossRef]
76. Gazetas, G. Vibrational characteristics of soil deposits with variable wave velocity. *Int. J. Numer. Anal. Methods Géoméch.* **1982**, *6*, 1–20. [CrossRef]
77. Taylor, C.A.; Dar, A.R.; Crewe, A.J. Shaking Table modelling of seismic geotechnical problems. In Proceedings of the 10th European Conference on Earthquake Engineers, Vienna, Austria, 28 August–2 September 1995; pp. 441–446.
78. Tao, X.; Kagawa, T.; Minowa, C.; Abe, A. Verification of dynamic soil-pile interaction. In *Geotechnical Earthquake Engineering and Soil Dynamics III*; Dakoulas, P., Yegian, M.K., Holtz, R.D., Eds.; ASCE: Reston, VA, USA, 1998; pp. 1199–1210.
79. Jakrapiyanun, W. Physical Modelling of Dynamics Soil-Foundation-Structure Interaction using a Laminar Container. Ph.D. Thesis, University of California, San Diego, CA, USA, 2002.
80. Prasad, S.; Towhata, I.; Chandradhara, G.; Nanjundaswamy, P. Shaking table tests in earthquake geotechnical engineering. *Curr. Sci.* **2004**, *87*, 1398–1404.

81. Tang, L.; Ling, X.; Xu, P.; Gao, X.; Wang, D. Shake table test of soil-pile groups-bridge structure interaction in liquefiable ground. *Earthq. Eng. Eng. Vib.* **2010**, *9*, 39–50. [CrossRef]
82. Chen, J.; Shi, X.; Li, J. Shaking table test of utility tunnel under non-uniform earthquake wave excitation. *Soil Dyn. Earthq. Eng.* **2010**, *30*, 1400–1416. [CrossRef]
83. Lee, C.-J.; Wei, Y.C.; Kuo, Y.C. Boundary effects of a laminar container in centrifuge shaking table tests. *Soil Dyn. Earthq. Eng.* **2012**, *34*, 37–51. [CrossRef]
84. Massimino, M.R.; Maugeri, M. Physical modelling of shaking table tests on dynamic soil–foundation interaction and numerical and analytical simulation. *Soil Dyn. Earthq. Eng.* **2013**, *49*, 1–18. [CrossRef]
85. Kumar, M.; Mishra, S.S. Study of seismic response characteristics of building frame models using shake table test and considering soil–structure interaction. *Asian J. Civ. Eng.* **2019**, *20*, 409–419. [CrossRef]
86. Kramer, S.L. *Geotechnical Earthquake Engineering*; Prentice Hall: Upper Saddle River, NJ, USA, 1996.
87. Kumar, A.; Choudhary, D.; Katzenbach, R. Effect of Earthquake on Combined Pile–Raft Foundation. *Int. J. Géoméch.* **2016**, *16*, 04016013. [CrossRef]
88. Gohl, W.B.; Finn, W.D.L. Seismic response of single piles in shaking table studies. In Proceedings of the 5th Canadian Conference on Earthquake Engineering, Ottawa, ON, Canada, 6–8 July 1987; pp. 435–444.
89. Valsangkar, A.; Dawe, J.; Mita, K. *Shake Table Studies of Seismic Response of Single Partially Supported Piles*; University of Toronto: Toronto, ON, Canada, 1991; pp. 327–334. [CrossRef]
90. Chandrasekaran, S.S.; Boominathan, A.; Dodagoudar, G.R. Dynamic Response of Laterally Loaded Pile Groups in Clay. *J. Earthq. Eng.* **2012**, *17*, 33–53. [CrossRef]
91. Sulaeman, N. The Use of Lightweight Concrete Piles for Deep Foundation on Soft Soils. Ph.D. Thesis, University in Tun Hussein Onn, Johor, Malaysia, 2010.
92. *IS 2062*; Hot Rolled Medium and High Tensile Structural Steel—Specification. Bureau of Indian Standards: New Delhi, India, 2011.
93. Salgado, R. The mechanics of cone penetration: Contributions from experimental and theoretical studies. In *Geotechnical and Geophysical Site Characterization 4 (ISC-4)*; CRC Press: London, UK, 2012; pp. 131–135. [CrossRef]
94. Memar, M.; Zomorodian, S.M.A.; Vakili, A.M. Effect of pile cross-section shape on pile group behaviour under lateral loading in sand. *Int. J. Phys. Model. Geotech.* **2020**, *20*, 308–319. [CrossRef]
95. Bao, Y.; Ye, G.; Ye, B.; Zhang, F. Seismic evaluation of soil–foundation–superstructure system considering geometry and material nonlinearities of both soils and structures. *Soils Found.* **2012**, *52*, 257–278. [CrossRef]
96. Kanaujia, V.K.; Ayothiraman, R.; Matsagar, V.A. Influence of superstructure flexibility on seismic response of pile foundation in sand. In Proceedings of the 15th World Conference on Earthquake Engineering, Lisboa, Portugal, 24–28 September 2012.
97. Paz, M. *Structural Dynamics—Theory and Computation*; CBS Publishers and Distributers Pvt. Ltd.: New Delhi, India, 2004.
98. Holzner, S. *Physics for Dummies*; Wiley Publishing, Inc.: Indianapolis, IN, USA, 2006.
99. Boominathan, A.; Ayothiraman, R. Measurement and Analysis of Horizontal Vibration Response of Pile Foundations. *Shock Vib.* **2007**, *14*, 89–106. [CrossRef]
100. Durante, M.G.; Di Sarno, L.; Mylonakis, G.; Taylor, C.A.; Simonelli, A.L. Soil-pile-structure interaction: Experimental outcomes from shaking table tests. *Earthq. Eng. Struct. Dyn.* **2015**, *45*, 1041–1061. [CrossRef]
101. Visuvasam, J.; Chandrasekaran, S.S. Effect of soil–pile–structure interaction on seismic behaviour of RC building frames. *Innov. Infrastruct. Solut.* **2019**, *4*, 45. [CrossRef]
102. American Society of Civil Engineers. *Minimum Design Loads and Associated Criteria for Buildings and Other Structures*; American Society of Civil Engineers: Reston, VA, USA, 2017.
103. Council, Building Seismic Safety. *NEHRP Guidelines for the Seismic Rehabilitation of Buildings: Prepared for the Building Seismic Safety Council*; FEMA: Washington, DC, USA, 1997.